



Long-term Effect of Metallic Iron Sorbents on Arsenic Mobility in an Anoxic Aquifer

– An assessment based on long-term column experiments

Långsiktig effekt av nollvärda järn-sorbenter på arseniks mobilitet i en anoxisk akvifer – en evaluering baserad på långtids-kolonnförsök

Stephanie Nyström

Degree project/Independent project • (30 hp)
Swedish University of Agricultural Sciences,
SLU Department of Soil and Environment
Soil and Water Management
Examensarbeten, Institutionen för mark och
miljö, SLU, 2022:14
Uppsala 2022



Long-term effect of metallic iron sorbents on arsenic mobility in an anoxic aquifer – An assessment based on long-term column experiments

Långsiktig effekt av nollvärda järn-sorbenter på arseniks mobilitet i en anoxisk akvifär – en evaluering baserad på långtids-kolonnförsök

Stephanie Nyström

Supervisor: Geert Cornelis, SLU, department of Soil and Environment
Assistant supervisor: Thiago Formentini, SLU, department of Soil and Environment
Assistant supervisor: Dan Berggren Kleja, SLU, department of Soil and Environment
Examiner: Jon Petter Gustafsson, SLU, department of Soil and Environment

Credits: 30 hp
Level: Advanced, A2E
Course title: Master thesis in Environmental science
Course code: EX0897
Programme/education: Soil and Water Management
Course coordinating dept: Department of Aquatic Sciences and Assessment

Place of publication: Uppsala
Year of publication: 2022
Cover picture: Stephanie Nyström
Title of series: Examensarbeten, Institutionen för mark och miljö, SLU
Part number: 2022:14

Keywords: Zero valent iron, ZVI, Remediation, Anoxic, Column tests, ICP-MS

Swedish University of Agricultural Sciences

Faculty of Natural Resources and Agricultural Sciences, NJ

Department of Soil and Environment

Unit/section (optional)

Publishing and archiving

Approved students' theses at SLU are published electronically. As a student, you have the copyright to your own work and need to approve the electronic publishing. If you check the box for **YES**, the full text (pdf file) and metadata will be visible and searchable online. If you check the box for **NO**, only the metadata and the abstract will be visible and searchable online. Nevertheless, when the document is uploaded it will still be archived as a digital file.

If you are more than one author you all need to agree on a decision. Read about SLU's publishing agreement here: <https://www.slu.se/en/subweb/library/publish-and-analyse/register-and-publish/agreement-for-publishing/>.

YES, I/we hereby give permission to publish the present thesis in accordance with the SLU agreement regarding the transfer of the right to publish a work.

NO, I/we do not give permission to publish the present work. The work will still be archived and its metadata and abstract will be visible and searchable.

Acknowledgements

I would like to thank my main supervisor Geert Cornelis and co-supervisor Thiago Formentini for all of your patient and warm support throughout this entire process, from teaching me the craft needed in the laboratory operations, to analysis of data and writing. Not only have you done your utmost to help me sharpen my scientific methods, but also offered a very nice and fun professional partnership. Further, I want to thank Dan Berggren Kleja who first invited me to write my thesis in this fascinating project, and who has been a positive and dedicated project head. Additionally, I would like to thank Mina Spångberg, Jan Fiedler and Oscar Skirfors for their support and nice collegueship in the laboratory. Lastly, I would like to thank Pär Hallgren at SWECO for welcoming us to and showing us around the grounds of the former impregnation plant at Hjärtevad.

Abstract

Zero valent iron (ZVI) sorbents have successfully remediated soils burdened with different groups of contaminants. When working to alleviate arsenic (As) contamination, the location-specific subsurface chemistry greatly affects the efficiency of the sorbents as it controls the speciation of As and the transformation of the ZVI, as well as the interaction between these (remediating mechanisms). Hence, planning for such full-scale remediation should suitably be based on lab-scale tests mimicking the in-field conditions of the site in question. In Hjärtevad, Sweden, wood impregnation practices with chromated copper arsenate (CCA) has contaminated an anoxic aquifer with As. In-field speciation of As has indicated that the expected form is dominating, which is the more mobile species As(III). This study aimed to test the long-term efficiency of different variants of commercially available ZVI towards As immobilization in the sediment from Hjärtevad, mimicking the on-site anoxic conditions and groundwater composition. Additionally, this study included an optimization of a method for analyzing sub $\mu\text{g L}^{-1}$ concentrations of As with inductively coupled plasma mass spectrometry (ICP-MS), and optimization of the column test design.

A long-term bottom-up flow column experiment containing sediment from Hjärtevad was performed, testing micro-sized ZVI, nano-sized ZVI and their sulfidated counterparts, each in a separate column. The eluates collected from the respective columns were compared with each other and previously performed batch tests of the same composition. The non-sulfidated sorbents showed better efficiency in the simulated Hjärtevad conditions in both column and batch tests. Both nano-sized sorbents initially increased mobilization of As from the column system, before shifting to an immobilizing phase. Increased pH and decreased redox potential in the eluates from all sorbent-treated columns in comparison with non-treated columns indicated corrosion of the ZVI core. This study suggests the micro-sized ZVI (Ferox Target, Hepure) for Hjärtevad, as it performed the best in the long-term column tests (99.7 % retention of the column As). Reaction mode with O_2 was found as the optimal method to analyze sub $\mu\text{g L}^{-1}$ concentrations of As with ICP-MS. Column experiments with sandy sediment testing ZVI performance for As was found to work well by replacing the provided filters with 70 μm Nylon mesh filter and without inducing aggregation of the sorbents with NaCl.

Keywords: Zero valent iron, ZVI, Remediation, Anoxic, Column tests, ICP-MS

Sammanfattning

Nollvärdiga järn-sorbenter (ZVI) har med god framgång avhjälpt kontaminering av olika grupper av markföroreningar. Vid tillfällen denna åtgärd riktas mot arsenikförorening är den platspecifika markkemin styrande i effektiviteten av sorbenten då den inte bara styr specieringen av arsenik (As) utan även omvandlingen av sorbenten, såväl som interaktionen mellan dessa (de åtgärdande mekanismerna). Därmed bör planering för fullskaliga saneringar av denna typ lämpligen föregås av tester i laboratorieskala som efterliknar fältförhållandena på platsen i fråga. I Hjärtevad har träimpregnering med kromerat koppararsenat (CCA) förorenat en anoxisk akvifär med As. Speciering av As i fält har indikerat att den förväntade As(III)-formen dominerar, som också är relativt mobil. Denna studie syftade till att testa den långsiktiga effektiviteten av olika varianter av kommersiellt tillgängligt ZVI när det gäller dess kapacitet för As-immobilisering i sediment från Hjärtevad, med återskapande av de anoxiska förhållandena och grundvatten-kompositionen i marken på platsen. Dessutom omfattar denna studie en optimering av en metod för att analysera sub $\mu\text{g L}^{-1}$ -koncentrationer av As med induktivt kopplad plasma mass-spektrometri (ICP-MS), och optimering av kolonnstestdesign.

Ett långtidsexperiment med kolonner med uppåtriktat flöde innehållande sediment från Hjärtevad genomfördes för att testa mikro-dimensionerad ZVI, nano-dimensionerad ZVI och deras sulfiderade motsvarigheter, i separata kolonner. Eluenterna som samlats från respektive kolonn jämfördes med varandra och med tidigare genomförda skaktester med samma sammansättningar. De icke-sulfiderade sorbenterna uppvisade bättre effektivitet i de simulerade Hjärtevad-förhållandena i både kolonn- och skak-test. Bägge nano-sorbenter ökade till en början mobiliseringen av As från kolonnerna innan de övergick till en immobiliserande fas. Ökat pH och minskad redox-potential i eluenten från samtliga sorbent-behandlade kolonner i jämförelse med icke-behandlade kolonner indikerade korrosion av ZVI-kärnan. I denna studie förordas den mikro-dimensionerade ZVI (Ferox Target, Hepure) för Hjärtevad, då den presterade bäst i långtids-kolonnförsöken (99.7 % retention av kolonnens As). Reaktions-läge med O_2 fastställdes som den optimala metoden för att analysera sub- $\mu\text{g L}^{-1}$ -koncentrationer av As med ICP-MS. Kolonn-experimentet med sandigt sediment för test av ZVI för As-sanering visade sig fungera bra genom att ersätta de medföljande filtren med 70 μm Nylon-nätfilter och utan att inducera aggregering av sorbenterna med NaCl.

Nyckelord: Nollvärdigt järn, ZVI, Sanering, Anoxisk, Kolonn-test, ICP-MS

Popular scientific summary

For a hunter or fisher, a traditional multitool might be an obvious companion, but imagine a similarly versatile tool in the hands of a specialist planning a remediation project of a contaminated site. Such a tool does in fact exist, in the form of a granular product made out of iron, called Zero-Valent Iron (ZVI). ZVI is not only a multitool in the way that it defuses contaminants in various ways: as a superglue, holding it in place at the contaminated site or transforming it to a less toxic compound, but also in the way that it can target several types of contaminants. One of these contaminants is the highly toxic element arsenic (As). Its main exposure path to humans is via groundwaters containing elevated levels, and this is why efforts are being made in order to prevent spreading of As through soils to these reserves or treating groundwater resources that are already contaminated. One of the main anthropogenic sources of As pollution is wood impregnation practices using chromated copper arsenate (CCA), and such an operation was active in Hjärtevad, Sweden in the 1900's, leaving behind very high volumes of As in the soil. Despite previous efforts to remediate the site, new ventures are being planned due to the still high levels at the site. Based on promising lab-scale test results of As-remediation with ZVI in recent years, this sparked the framework for the new venture, which would allow remediation through adding the ZVI to the soil. This study is part of a series of lab-scale tests branching out the details of the continued Hjärtevad remediation. Its contribution consisted of a long-term experiment testing the efficiency of four different commercially available ZVI in remediating the contaminated soil from Hjärtevad, targeting As. The experiment was performed using columns that fix the soil and ZVI in place while letting artificial groundwater being pumped through, mimicking a section of the subsoil treated by ZVI at the site being naturally percolated with groundwater. Part of the study was to optimize the setup design for these columns, and also optimize the settings for the analytical tool used to detect the leached As concentrations from the columns. Apart from using actual soil from Hjärtevad and artificial groundwater mimicking the composition at the site, the experiment was performed in an atmosphere with very low O₂ concentration, all to represent field conditions as well as possible. The ZVIs that were tested were micro-sized and nano-sized ZVI as well as their sulfide-covered counterparts. The long-term remediation efficiency towards As in the mimicked Hjärtevad conditions was the highest for the micro-sized ZVI, retaining 99.7% of

its initial As-input. Hence, this sorbent is suggested as part of the future Hjärtevad venture. Though this assessment was purely based on immobilizing capacity, hence excluding mobility challenges during the delivery of the product into the soil. For the final choice of ZVI for Hjärtevad, the mobility of the products should be assessed.

Remediation in Sweden is planned and performed in a systematic way, though the experience and knowledge about ZVI application in Swedish soil is sparse. The methods that are continuously chosen, due to recognition and previous practice, are rather commonly demanding an initial excavation of the contaminated body, making many remediation projects labour intensive. Expanding the knowledge in the Swedish context of more innovative techniques like ZVI, which can be added directly to the contaminated body, builds the foundation for future remediation being more cost- and labour-efficient and even better aimed for the specific location due to the wider variety of options.

Table of contents

List of tables	12
List of figures.....	13
Abbreviations	15
1. Introduction.....	18
1.1. Contaminated sites Sweden.....	18
1.2. Arsenic in nature.....	19
1.3. Soil remediation for arsenic	20
1.4. Motivation of the current study	21
2. Theoretical background.....	22
2.1. Geochemistry of arsenic.....	22
2.2. Zerovalent Iron	24
2.2.1. Remediative Arsenic-Zerovalent Iron reactions.....	25
2.2.2. Environmental factors regulating Arsenic Immobilization	27
2.2.3. Zero valent iron properties and modifications.....	28
2.3. ICP-MS analysis of As.....	30
2.3.1. Working principle of ICP-MS.....	30
2.3.2. Internal standard	30
2.3.3. Interferences	30
2.4. Column and batch testing.....	32
2.4.1. Comparison column and batch tests	32
2.4.2. Preliminary studies of Hjaltevad - batch tests.....	34
3. Material & methods	37
3.1. Site description	37
3.2. Sediment sampling	39
3.4. Sorbents	40
3.5. Column experiments.....	41
3.5.1. Artificial groundwater	42
3.5.2. Packing procedure and percolation	42

3.5.3.	Preparatory experiment: Sorbent retention – No system manipulation	
	43	
3.5.4.	Preparatory experiment: Sorbent retention - Addition of NaCl	44
3.5.5.	Preparatory experiment: Short term leaching	45
3.5.6.	Long-term experiment.....	45
3.6.	Microwave-assisted digestion	48
3.7.	Elemental Analysis	48
4.	Results.....	50
4.1.	ICP-MS method optimization.....	50
4.2.	Column protocol development.....	50
4.3.	Long-term column leaching	50
4.3.1.	Iron.....	51
4.3.2.	pH and Redox Potential (Eh).....	55
4.3.3.	Arsenic	57
5.	Discussion.....	63
5.1.	ICP-MS method development	63
5.2.	Trends of column leaching, pH and Eh as compared to batch tests.....	63
5.2.1.	Reference	63
5.2.2.	S-mZVI.....	64
5.2.3.	S-nZVI.....	65
5.2.4.	mZVI	66
5.2.5.	nZVI	66
5.3.	Long-term reactivity of sorbents toward As(III) and As(V)	67
5.4.	Suggested mechanisms for mZVI, nZVI and S-nZVI	68
6.	Conclusions	71
	References	72

List of tables

Table 1. Characteristics of ZVI sorbents used in the column experiments.	41
Table 2. Salts, their respective stock concentrations and amounts used for AGW preparation.	42
Table 3. Content of columns and procedure for mixing in the sorbents.....	45
Table 4. Concentration of Fe in commercial ZVI, mass used for preparation of sorbent packing phase, and its final amount & Fe concentration.....	46
Table 5. Mass balance for leached Fe for the entire experiment duration for each column type.	54
Table 6. Mass balance for leached As for the entire experiment duration for each column type.	61

List of figures

- Figure 1. Eh-pH stability diagram for the dominant As aqueous species at equilibrium. At 25° C with a total dissolved As concentration of 10^{-6} mol L⁻¹. Redox potential shown in reference to the standard hydrogen electrode, SHE and in V, on y-axis. As(V) species shown in green (higher redox potential), As(III) species shown in yellow (lower redox potential). Diagram produced by author, using Spana©, Ignasi Puigdomenech, available at <https://sites.google.com/site/chemdiagr/home>.23
- Figure 2. Results from up to 30 days batch tests. A_{TOT} and As(III) concentrations in solution shown in $\mu\text{g L}^{-1}$ to the left. Note the scale difference of the y-axis for the batch system without sorbent. Eh shown mV and pH values for respective batch systems to the right.36
- Figure 3. The area of the former impregnation plant in Hjärtevad. Also shown is the position of the former storage tank of the impregnation solution, deep shaft and sampling points for sediment and ground water. Standardkartan © OpenStreetMap contributors, licensed under CC BY-SA 2.0.37
- Figure 4. Stability diagram for As showing pH-redox-regions where As(III) and As(V) species are prevalent. Blue dots are measured pH and Eh in the soil at the site in Hjärtevad in the years 2016-2018 (SWECO 2019, p. 94).39
- Figure 5. Packing of columns. Photos taken by author.43
- Figure 6. Preparatory column-experiment inside glove box. Photo taken by author.44
- Figure 7. Long-term column experiment setup shown for one column. All 10 columns were simultaneously provided with AGW from the same eluent container with the same peristaltic pump. Eluate was collected in 10 separate containers.46
- Figure 8. Long-term experiment columns with their respective eluate containers inside the glove box. Shown in the foreground is the collective AGW container. Photo taken by the author.47
- Figure 9. Sampling flow chart for long-term column experiment.48
- Figure 10. Fe leaching per respective column type in mg L^{-1} . Fe_{TOT} from respective duplicate shown in red squares and $< 0.45 \mu\text{m}$ fraction from respective duplicate shown in blue circles. Time of experiment duration is expressed in number of pore volumes passed through respective column type.51

Figure 11. pH (purple and left y-axis) and Eh in mV (green and right y-axis) measured in eluates from respective column type. Time of experiment duration is expressed in number of pore volumes passed through respective column type.	55
Figure 12. As leaching per respective column type in $\mu\text{g L}^{-1}$. As_{TOT} from respective duplicate shown in red squares, $< 0.45 \mu\text{m}$ fraction from respective duplicate shown in blue circles and As(III) from respective duplicate shown in green triangles. Time of experiment duration is expressed in number of pore volumes passed through respective column type. Samplings are marked with grey numbers 1-12.	57
Figure 13. Total amount of leached As during the experiment per column type. Each As fraction amount expressed in % in relation to the corresponding leached amount from the reference duplicates.	62

Abbreviations

AGW	Artificial groundwater
Al	Aluminum
Ar	Argon
ArCl ⁺	Argon chloride ion
As	Arsenic
As(0)	Elemental arsenic
As(III)	Arsenite
As(V)	Arsenate
As ⁺	Monovalent arsenic
As ₂ S ₃	Arsenic trisulfide
AsO ₄ ³⁻	Arsenate ion
As _{TOT}	Total arsenic content
CaCl ⁺	Calcium chloride ion
CaCl ₂	Calcium chloride
CCA	Chromated copper arsenate
C _{Fe}	Concentration of iron
Cl ⁻	Chloride
CMC	Carboxymethylcellulose
CO ₃ ²⁻	Carbonate
Cps	Counts per second
Cr	Chromium
DW	Dry weight
Eh	Redox potential
ENM	Engineered nanomaterials
EPA	Environmental protection agency
Fe	Iron

Fe(0)	Zero valent iron
Fe(II)	Divalent iron
Fe(III)	Trivalent iron
Fe ²⁺	Divalent iron ions in solution
FeS	Iron sulfide
Fe _{TOT}	Total iron content
H ₂	Hydrogen gas
H ₂ PO ₄ ⁻	Dihydrogen Phosphate
HCl	Hydrochloric acid
HCO ₃ ⁻	Hydrogencarbonate
He	Helium
HNO ₃	Nitric acid
ICP-MS	Inductively coupled plasma mass spectrometry
K _d	Partitioning coefficient
KED	Kinetic energy discrimination
Kr	Krypton
LOD	Detection limit
LOQ	Limit of quantification
m/z ⁺	Mass-to-charge ratio
Mn	Manganese
Mo	Molybdenum
mZVI	Micro zero valent iron
N ₂	Nitrogen gas
nZVI	Nano zero valent iron
O ₂	Oxygen
PAA	Polyacrylic acid
PAH	Polycyclic aromatic hydrocarbon
PO ₄ ³⁻	Phosphate
PV	Pore volume(s)
Re	Rhenium
RH 2000	The Swedish national height system 2000
S	Sulfide

Sb	Antimony
Se	Selenium
SGI	Swedish geotechnical institute
SiO_3^{2-}	Silicate
SO_4^{2-}	Sulphate
S-ZVI	Sulfidated zero valent iron
Tc	Technetium
ZVI	Zero valent iron

1. Introduction

1.1. Contaminated sites Sweden

Ca. 80 000 contaminated or potentially contaminated sites have been identified in Sweden and ca. 9000 of these are considered being of high to very high risk of causing harm to human health and environment (Naturvårdsverket 2021). Previous sites of glassworks, dry cleaning, mining, pulp & paper industry and different functions for the wood industry are commonly listed among these prioritized objects, having released contaminants such as heavy metal(loid)s, petroleum products, dioxins and PAHs (Naturvårdsverket 2022b). The assessment of these industrial sites was performed the years 1999-2015, followed by a period of organizing remediation of them (Naturvårdsverket 2022a). So far, approximately 3000 state funded remediation projects have been finalized, and a similar number of projects are currently ongoing (Naturvårdsverket 2022c).

The dominating remediative action in Sweden has been excavation of contaminated masses (such as soil), unless the site in question poses technical challenges for this alternative (Helldén et al. 2006, Vestin et al. 2021). The main challenge for this has been technical difficulties in performing the excavation at the site (Vestin et al 2021). An *in-situ* method that has commonly been used is vacuum extraction/soil venting. This is a concentration/enrichment-method that aims to, post extraction, result in a mass with condensed concentration of the contaminant that can be controlled and contained. Vacuum pumps are used to create a negative pressure in the contaminated subsurface, inducing a flow of the mass which allows its extraction. Once on the surface, the contaminant can be treated with for example filters of activated carbon. The method can be complemented with heated air added to the extraction pipes, increasing the volatility of the mass, hence the at times designation “soil venting” (Helldén et al. 2006). Other *in-situ* solutions that have been applied are bio-attenuation, barriers and filters (Helldén et al. 2006).

Stakeholders within remediation of Sweden testify to a prevailing lack of knowledge and practical experience of remediation techniques other than excavation (Vestin et al. 2021). A shift from the resource-intensive excavation- and

deposition alternative towards for example *in-situ* methods could increase the overall environmental benefit of the remediation actions that are taken (SGU 2021).

As a part of the Swedish EPA aims to increase the rate of remediating contaminated sites, they have recently started to systematically prioritize applications for funding of projects that include innovative techniques of remediation (Naturvårdsverket 2021). A research-oriented equivalent is TUFFO, a program run by the Swedish Geotechnical Institute (SGI) to increase the remediation rate of contaminated sites by promoting research in these techniques and decreasing the gap between this research and the practical on-site remediation (SGI 2020).

1.2. Arsenic in nature

Arsenic (As) is the 20th most abundant element in the Earth's crust, and this metalloid is found in soils and waters both by natural and anthropogenic causes (SGU 2022, Kemakta Konsult AB & Institutet för Miljömedicin 2011, Wenzel 2013). Compounds containing As are highly toxic to humans and the main exposure path is through drinking water (WHO 2019). The As presence in groundwater is therefore of high concern (Kanel et al 2005).

Geologically, As occurs mainly in sulphide ores, the most abundant of them being arsenopyrite (FeAsS) (Smedley and Kinniburgh 2002). The major natural input of As to soils is through weathering of these As-containing rocks. Atmospheric deposition is also a large flux of As to soils, though the dominating contributors are anthropogenic as the atmospheric deposition is larger in proximity to urban areas and mining related areas (Wenzel 2013). Estimations of global As cycling shows a positive net balance for the soil pool, i.e. the net input of As (via e.g. atmospheric deposition and weathering) is larger than the output of As from soils, via e.g. erosion or leaching. This makes soils a major storage compartment for As, with a retention time of 1000-3000 years due to the anthropogenic input and generally low mobility of As in soils. The global average concentration of As in soils is estimated to range between 5 and 7.5 mg kg⁻¹ (Wenzel 2013). The main anthropogenic sources of As pollution in soils are different parts of the mining industry, sites of preparation and final use of wood impregnated with chromated copper arsenate (CCA) and fossil fuel combustion (Wenzel 2013, Smedley and Kinniburgh 2002).

The global background concentration of As in groundwater is estimated between 0.5 and 0.9 µg L⁻¹ (Wenzel 2013). Groundwaters with naturally elevated As concentrations are mainly found in closed basins in arid and semi-arid areas with high pH or strongly reducing aquifers where low water flow and young sediments cause As to accumulate. Many of these groundwater sources reach As concentrations > 100 µg L⁻¹, some groundwaters even exceed several thousands µg

L⁻¹ (Smedley and Kinniburgh 2002). These values exceed the Swedish guideline value for As in groundwater, which is 5 µg L⁻¹. For drinking water it is 10 µg L⁻¹ (Kemakta Konsult AB & Institutet för Miljömedicin 2011).

Once in water and soils, As mainly occurs in two forms: As(III) (arsenite) and As(V) (arsenate), the former dominating in reducing conditions and the latter in oxidizing (WHO 2019). As(III) is the most toxic and mobile of the two. This has important consequences for As remediation. Note that As geochemistry is discussed in more detail in the theoretical section (2.1).

1.3. Soil remediation for arsenic

Different methods have been tested to alleviate As contamination of aquifers and other bodies of water. Addition of sorbents stands out by showing great promise with its simple application, high removal efficiency of As and low cost. Iron-based sorbents such as zero valent iron (ZVI) carry the additional advantage by being an environmentally harmless and relatively cheaply produced material (Tuček et al. 2017, Mondino et al. 2020).

ZVI sorbents are a group of sorbents with different compositions and sizes such as microsized ZVI (mZVI), nanosized ZVI (nZVI), oxidic shell free ZVI (OSF-ZVI) and sulfidated ZVI (S-ZVI). They are often produced or injected to contaminated bodies together with organic surface modifiers such as carboxymethylcellulose (CMC) and polyacrylic acid (PAA) (Liu et al. 2015). The sorbent immobilizes and/or transforms the contaminant to a less toxic compound, with mechanisms differing according to sorbent modification and environmental conditions (more detail in section 2.2).

ZVI is used through direct treatment of the contaminant source zone or by targeting the groundwater leaching from the contaminant source using permeable reactive barriers. The former alternative can be done *in-situ* by high pressure injections by direct push or low-pressure hydrodynamic injection using screened wells. The injections add the ZVI as a slurry with water. *Ex-situ* source treatment entails excavation followed by ZVI treatment of the contaminated mass (Mondino et al. 2020).

ZVI has been applied to contaminated groundwater and various types of wastewater, in lab-, pilot- and field-scale though most research has been done in lab scale (Li et al. 2014, Wang et al. 2021, Kumpiene et al. 2021, Tuček et al. 2017, O'Carroll et al 2013). It has been proven efficient for the removal of contaminants such as chlorinated solvents, metalloids such as As, chromium (Cr), antimony (Sb), technetium (Tc), rhenium (Re), molybdenum (Mo) (Wang et al 2021, O'Carroll et al 2013).

The different modifications of the ZVI lead to different advantages and drawbacks. The more recently developed nZVI is generally more reactive towards

contaminants as compared to the mZVI, owing to its higher specific surface area (Schmid et al 2015, Li et al 2014). The mZVI on the other hand comes with the advantage of longer lifespan, lower cost and easier and safer use due to the dry state of the product (Mondino et al 2020). S-ZVI has shown long life span and efficient As removal, with S-nZVI efficiently removing As(III) under anoxic conditions (Fan et al 2017, Wu et al 2018). Sulfide coating has helped stabilize nano-sized ZVI solutions that in its pristine form can express colloidal behavior. This counteracted aggregation enhances the availability of the main efficiency-advantage of the nano-sized ZVI: its high specific surface area (Li et al 2006, Wu et al 2018). Beyond this, the sulfide coating causes a more irregular surface than for the pristine ZVI in solution, increasing the reactive surface area and therefore sorbent efficiency even more (Wu et al 2018). The efficiency of As removal by mZVI and nZVI is well-investigated in different controlled conditions, for example both oxidizing and reducing, and the nZVI removal efficiency has been shown as high as average 239 mg As g⁻¹ Fe on pilot scale (Yuan & Lien 2006, Li et al. 2014, Cheng et al. 2021, Gil-Díaz et al. 2016, Wang et al. 2021, Zou et al. 2016).

1.4. Motivation of the current study

This report is part of a series of lab- and field studies focusing on a CCA-contaminated site in Hjärtevad (Småland), Sweden. A batch test study was concluded prior to this study where the As sorption efficiency of S-nZVI, nZVI, S-mZVI and mZVI from the Hjärtevad soil was studied under anoxic conditions, that mimic the conditions of the contaminated soil layer in the field. The present study also mimics field conditions, but in the form of percolation experiment in columns with the same sorbents, sediment and also anoxic conditions.

The purpose of this study is to investigate the long-term efficiency of these 4 different commercial sorbents of immobilizing As in the sediment. It is hypothesized that the sulfidated ZVI are more efficient in immobilizing As than their non-sulfidated counterparts. The products are NANO FER 25DS from NANO IRON (S-nZVI), NANO FER 25S from NANO IRON (nZVI), S-MicroZVI from REGENESIS (S-mZVI) and Ferox Target from Hepure (mZVI). As outlined further, a flow-through column set-up creates more realistic conditions than a batch test. This study comprises first an optimization of a method for analyzing sub µg L⁻¹ concentrations of As with inductively coupled plasma mass spectrometry (ICP-MS). Then, several experiments are reported to optimize the column test design. Finally, the long-term column experiments are reported, where the efficiency of the different sorbents is compared.

2. Theoretical background

2.1. Geochemistry of arsenic

In nature, As is found in the redox states -III, 0, +III and +V, though in the most common conditions of groundwater and unsaturated soil pore water, As(III) and As(V) dominate (Wenzel 2013, Bowell et al 2014). Their inorganic aqueous species exist as oxyanions with charge and stability governed by pH and redox potential of the solution (Wenzel 2013). Thermodynamic predictions of the stability zones of As state that As(V) will dominate in oxidizing conditions and/or high pH, and As(III) in reducing conditions and/or low pH (Sadiq 1997)(Figure 1). At the pH values of most soil porewaters (3-9), in oxidizing conditions, As(V) is prevalent in its negatively charged species H_2AsO_4^- or HAsO_4^{2-} (Wenzel 2013). The pK_a values for the deprotonation of the As(V) oxyanions are: $\text{pK}_{a1} = 2.2$, $\text{pK}_{a2} = 6.9$ and $\text{pK}_{a3} = 11.5$ (Wang and Mulligan 2006). In anaerobic conditions below pH 9.2, the more toxic As(III) dominates as the neutrally charged H_3AsO_3^0 (Kanel et al 2005). This is explained by the pK_a values of the oxyanions of As(III): $\text{pK}_{a1} = 9.2$ and $\text{pK}_{a2} = 12.1$ (Wang and Mulligan 2006). It should be noted that natural systems are more complex than these idealized predominance diagrams, for example: oxidation of As(III) to As(V) is a kinetically slow process, which can lead to co-existence of these redox states even in oxidizing conditions (Wang and Mulligan 2006).

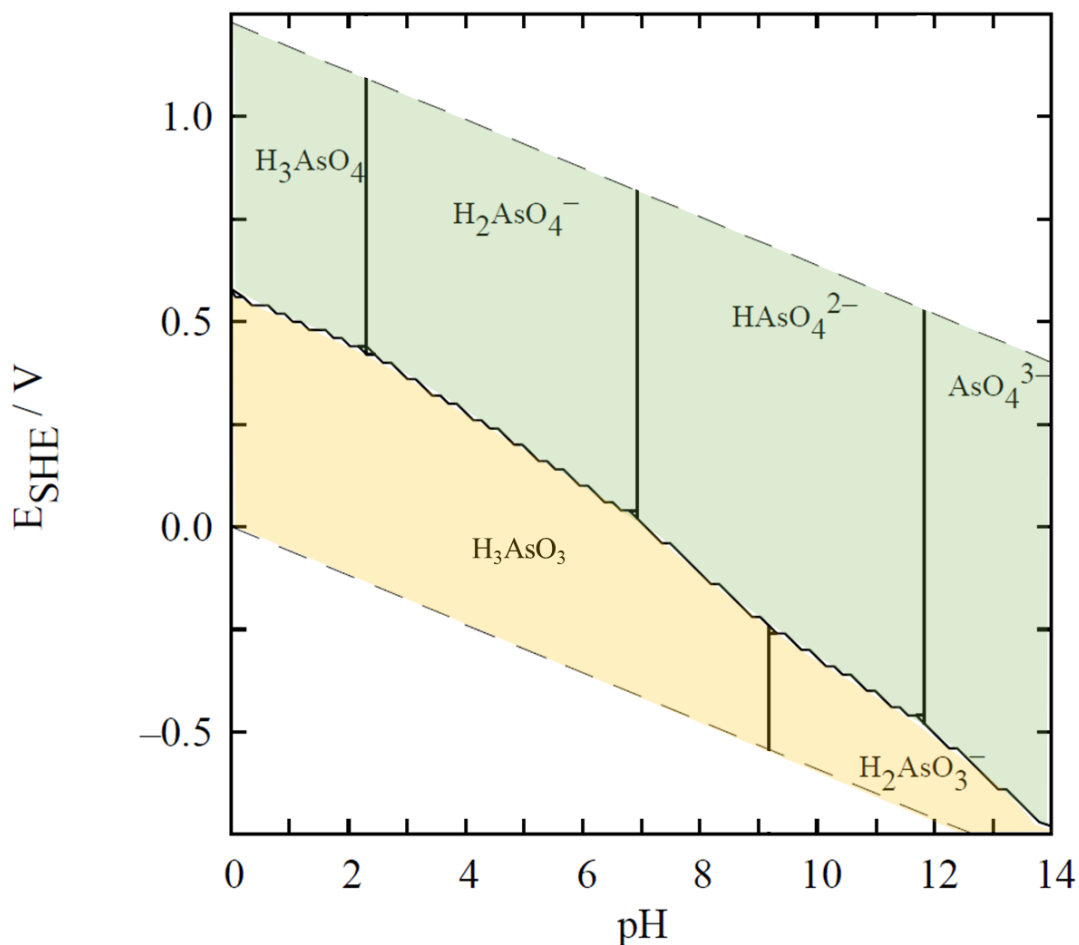


Figure 1. Eh-pH stability diagram for the dominant As aqueous species at equilibrium. At 25° C with a total dissolved As concentration of 10^{-6} mol L $^{-1}$. Redox potential shown in reference to the standard hydrogen electrode, SHE and in V, on y-axis. As(V) species shown in green (higher redox potential), As(III) species shown in yellow (lower redox potential). Diagram produced by author, using Spana©, Ignasi Puigdomenech, available at <https://sites.google.com/site/chemdiagr/home>.

The charge of the aqueous As species is the primary control of As mobility in soils, because through varying electrostatic attraction or repulsion, it determines the differing sorption affinity of these species, mainly to Fe-(hydr)oxides (Kanel et al 2005, Wenzel 2013). Sorption to aluminum (Al)- and manganese (Mn)-oxide-surfaces by As(III) and As(V) also occurs, though with weaker associations. Association with Fe(hydr)oxides tends to dominate even when these other oxides are present (Martin et al 2014, Wenzel 2013).

The aqueous As species form mainly inner-sphere complexes with the OH-functional groups of Fe-(hydr)oxide surfaces (Wang and Mulligan 2006), but because of the neutral charge of H_3AsO_3^0 , As(III) does not associate as strongly with Fe-(hydr)oxides as the negatively charged As(V) species. As(III) is therefore more mobile in soils (Wang and Mulligan 2006). Both As(V) and As(III) form bidentate binuclear with Fe-(hydr)oxides (Wang and Mulligan 2006). The wide pH range of the predominance of the uncharged As(III) oxyanion has important

consequences for As mobility in soils. The sorption maximum for As(III) occurs at pH 7-9, and for As(V) at pH 3-5. As the negative charge of the Fe(hydr)oxide functional groups increase with pH, so does the electrostatic repulsion between them and the negatively charged As(V) oxyanions. This favors desorption of As(V) at higher pH values (Wang and Mulligan 2006). Given that As(III) sorbs less strongly to Fe(hydr)oxides, colloidal mobilization of As(III) has been shown to be less important compared to As(V).

The partitioning coefficient, K_d , is commonly used in modeling of contaminant transport in the subsurface to quantify the ratio of a contaminant in the solid phase to that in solution. For As, the most interesting parameters for the K_d are the concentration of the subsurface As that is sorbed mostly to Fe(hydr)oxides and the concentration of the As in the soil solution (U.S. EPA 2004). The stronger the sorption, the more will the transport of the contaminant be retarded in relation to the groundwater flow (Smedley and Kinniburgh 2002). Because As(V) sorbs stronger to Fe(hydr)oxides than As(III), its K_d can generally be expected to be higher. K_d values for As presented median 3.3 for As(III) and 6.7 for As(V) (Baies and Sharp 1983 see Kuhlmeier 1997). In another study, for specifically natural hematite at neutral pH, K_d was found to be 21 for As(III) and 25 for As(V) (Bowell 1994). Generic K_d factors should be used with caution because many different aspects of the chemistry of the site will affect the partitioning of a contaminant, hence, lab tests to provide *site-specific* K_d values are encouraged (U.S. EPA 2004).

2.2. Zerovalent Iron

ZVI is a product of Fe particles which comes in variations in size, coatings and overall composition. ZVI can be synthesized by several different procedures. The most commonly used methods for nZVI synthesis are gas phase reduction and liquid phase reduction. This can entail reducing goethite and hematite particles with hydrogen gas (H_2) at high temperatures (O'Carroll et al 2013). Surface coating (such as sulfide), aiming to reduce the aggregation of nano-sized ZVI (see 2.2.3), can be added either pre- or post-synthesis (Yan et al 2013).

After ZVIs are transported into the contaminated subsurface with the appointed technology, via e.g. low-pressure injection, the sorbents are attached to the soil and/or spread out in the soil water. ZVI is then intended to transform the target contaminant to a less toxic and/or less mobile substance. ZVIs offer a wide assortment of possible immobilization mechanisms for several candidates and categories of contaminants (O'Carroll et al 2013). The mechanisms for As remediation by ZVI presented below occur in a sequence or as a parallel combination. The efficiency and dominance of mechanisms are governed by the properties of the sorbent and the geochemical environment in which they are applied (Wang et al 2021).

2.2.1. Remediative Arsenic-Zerovalent Iron reactions

As remediation by bare ZVI is primarily mediated through mechanisms of adsorption, coprecipitation and/or redox reactions (reactions with sulfidated ZVI are treated in a separate section further below). An important factor that has shown to affect these reactions is the corrosion of the ZVI surface that spontaneously occurs upon its addition to water (Wang et al 2021).

ZVI corrosion

The major providers of sorption sites for As are corrosion products (Fe (hydr)oxides) of ZVI which are spontaneously formed following reaction of ZVI with water (Wang et al 2021). The main mechanism of this Fe(hydr)oxide generation is oxidation of Fe(0) to Fe(III) and Fe(II). In oxic conditions, the dissolved O₂ acts as the oxidant, whereas in reducing conditions, H₂O is the oxidant. Following this oxidation of the surface of the ZVI, the Fe(III) and/or Fe(II) react with OH⁻, forming corrosion products on the ZVI surface, known as the oxidic shell of the ZVI. The Fe(hydr)oxide formation in oxic conditions is relatively rapid, while in anoxic conditions it is slower (Bang et al 2005a). Bang et al (2005b) observed the corrosion of Fe(0) filings in different conditions. At pH 7 in anoxic conditions, soluble and suspended Fe-hydroxide precipitates formed by the corrosion of the Fe(0) reached 5.3 mg L⁻¹ after 120 min of mixing with As(V). At pH 7 in oxic conditions, the total concentration of Fe in the As solution was about 11 mg L⁻¹ after 90 min of mixing.

The type of Fe(hydr)oxide that is formed varies with the chemical conditions: Green rusts, which are Fe(II)-Fe(III)-hydroxides, can be slowly formed upon oxidation of Fe(0) in reducing conditions at about pH 4-10 in the presence of Cl⁻. This group of minerals are considered intermediate phases because of their high sensitivity to oxidation in the open air. In this case, they are oxidized to either lepidocrocite (γ-FeOOH) or magnetite (Fe₃O₄). Which of these two minerals that is then formed, is dependent on oxidation rate and pH. A low oxidation rate favors magnetite formation (Randall et al 2001, Kumar et al 2014). Magnetite can also be slowly formed in anoxic conditions, on the ZVI surface (Bang et al 2005a, Usman et al 2018). Magnetite can be the main corrosion product in anoxic conditions (Wang et al 2021). Hematite (α-Fe₂O₃) can be formed in oxidizing conditions through oxidation of magnetite and is the end product of the oxidation chain (Dunlop and Özdemir 2015). Goethite (α-FeO·OH), a Fe(III)-hydroxide, can be formed in oxic conditions at high oxidation rates (Kumar et al 2014).

Due to its higher specific surface area, the corrosion and following Fe(hydr)oxide formation is more extensive for nZVI than that for mZVI (Shi et al 2015).

Common effects on a system where either oxic or anoxic corrosion of Fe(0) occurs are increase of pH, lowering of Eh and release of Fe²⁺. In anoxic conditions,

the increase of reducing conditions upon Fe(0) corrosion is even more prominent due to H₂ formation (Wang et al 2021).

Adsorption

The As immobilization by adsorption generally occurs more readily for As(V) than for As(III) species, because the association with Fe(hydr)oxides is generally stronger for the former (Wang et al 2021). Though this section goes into more detail to show in which environmental conditions the picture is not as straightforward.

Green rust has the ability to sorb As(V) by inner-sphere complexes, and these inner-sphere complexes have remained stable even following oxidation of the mineral to lepidocrocite (Randall et al 2001). As(V) sorb strongly to green rust and magnetite, and at neutral pH by inner-sphere complexes (Usman et al 2018).

As(III) forms inner-sphere complexes with magnetite (Hao et al 2018). The extent of As(III) sorption to magnetite increases from pH 3 to pH 9.5 (Dixit and Hering 2003). As indicated earlier (section 2.1), As(III) sorption to Fe(hydr)oxides is less pH dependent than that for As(V) (Bowell 1994).

Both As(V) and As(III) has been shown to sorb to a greater extent to goethite and lepidocrocite as compared to hematite. In pH 3-9 As(V) sorb to all of these minerals to a greater extent than As(III). Sorption maxima to these minerals are found in the pH range 6-8 for both As(V) and As(III) (Bowell 1994).

As(V) associates stronger to hematite than to goethite, by both inner- and outer-sphere complexation (Mamindy-Pajany et al 2011, Catalano et al 2008). For As(III), complexation with hematite is mainly occurring as inner-sphere type (Martin et al 2014). As(V) and As(III) sorb to goethite through inner-sphere complexes (Manning et al 1998, Martin et al 2014). Below pH 5-6 the sorption of As(V) to goethite is favored, while above pH 7-8 the affinity to As(III) is higher (Dixit and Hering 2003, Manning et al 1998).

The more ordered minerals, more “mature” in the group of Fe(0) corrosion products, goethite and hematite, have less specific surface area than the less ordered Fe(hydr)oxides and younger corrosion products such as lepidocrocite. This makes the efficiency for As(V) adsorption per mass of oxide lower for the former. The effect is not as pronounced for As(III) (Smedley and Kinniburgh 2002).

Coprecipitation

Coprecipitation emerges (mainly) from association between the ZVI corrosion products and As species, either directly with released Fe²⁺ or upon adsorption to precipitated or still ZVI-surface fixed Fe(hydr)oxides. An example of a solid phase that can precipitate in these cases is FeAsO₄ (Wang et al 2021). Coprecipitation on the ZVI surface leads to interlocking of the contaminant into the solid structure, hence forming a more stable immobilization than adsorption, which is occurring in the solid-solution-interface (Sun et al 2016). Thus, the adsorbed As can be

mobilized by pH changes and/or competing ions (see 2.2.2), and this is not likely to affect As-precipitates to the same extent. Though many As(V) surface complexes to Fe(hydr)oxides have been found to be irreversible adsorption reactions (Wang et al 2021).

Redox reactions

The reduction of As(III) and As(V) to lower redox states by Fe(0) is thermodynamically favorable (Wang et al 2021). Tuček et al (2017) found that OSF-nZVI had high removal capability of As(III) in anoxic conditions at lab-scale. They observed that As(III) was reduced to sparingly soluble As(0) by OSF-nZVI under anoxic conditions. Such a reduction can be mediated both by the Fe(0) core or by ambient H₂ (product of anoxic ZVI corrosion), both alternative pathways consuming protons. They further showed findings of firm locking of the As(0) into the Fe(0) core overlain by a minor shell of Fe(III)-oxide. Yan et al (2012) reported that As(III) reduction to As(0) was a trait only found for nZVI but not with mZVI.

The Fe²⁺ formed upon Fe(0) oxidation can also oxidize As(III) to As(V). This can then lead to increased amount of adsorbed As(V) to Fe(hydr)oxides, due to the stronger association for As(V) as compared to As(III) (section 2.1) (Wang et al 2021). Reduction of As(III) and As(V) by Fe(0) commonly results in increase in pH and Fe²⁺ concentration and decrease in Eh, as mentioned above (Wang et al 2021).

2.2.2. Environmental factors regulating Arsenic Immobilization

The main chemical regulators of the As immobilization by ZVI are dissolved O₂, pH, and co-existing anions (Wang et al 2021).

The dissolved O₂ concentration plays a key role in the efficiency of ZVI sorbents. Any environmental shifts favoring corrosion of the Fe(0) is likely to favor immobilization given the importance of corrosion products. As oxic corrosion of ZVI is much more rapid than anoxic corrosion (section 2.2.1), increased dissolved O₂ increases ZVI immobilization efficiency by creating much more adsorption sites, making adsorption the dominating mechanism. This effect is especially pronounced for As(V) immobilization due to its higher affinity to Fe(hydr)oxides. Due to slow ZVI corrosion in anoxic conditions (section 2.2.1), adsorption to Fe(hydr)oxides becomes a less important mechanism when the dissolved O₂ concentration is low. Hence, longer exposure time is needed for efficient adsorption (Wang et al 2021, Tanboonchuy et al 2011). Bang et al (2005a) observed that the slow oxidation in anoxic conditions generated insignificant amounts of precipitates in 9 hours, and rather lead to a gradual production of the soluble Fe(II).

Oxic conditions cause enhanced and rapid oxidation of As(III) to As(V) by dissolved O₂, but also by the large amount of Fe(hydr)oxides formed from the enhanced ZVI corrosion prevailing in oxic conditions (Wang et al 2021, Tuček et

al 2017, Manning et al 2002). Reduction of As(III) to As(0) by OSF-ZVI has been shown to be favored by anoxic conditions (Tuček et al 2017).

Sorption of As is largely dependent on pH, as explained in section 2.1 and 2.2.1. Similarly as for soil Fe(hydr)oxides, the surface charge of the ZVI particle changes with pH, being more positively charged at $\text{pH} < 7$ and more negatively charged at $\text{pH} > 7$ (Kanel et al 2005). This leads to enhanced adsorption in pH 2-7 of the negatively charged As(V) species (H_2AsO_4^-) to the positively charged ZVI surface due to electrostatic attraction. In pH 7-12, when the ZVI surface becomes more negatively charged, the interaction with the still negatively charged As(V) (HAsO_4^{2-}) leads to increased electrostatic repulsion and therefore decreased adsorption. In pH 4-7 the neutrally charged As(III) (H_3AsO_3^0) has shown adsorption to the positively charged ZVI, though above pH 7 where As(III) species are mainly negatively charged (H_2AsO_3^- or HAsO_3^{2-}), the electrostatic repulsion became great enough to the negatively charged ZVI for adsorption to be lowered (Tanboonchuy et al 2011).

Formation of Fe(III) hydroxide is favored at high pH systems. Therefore it is also favored by a system where Fe(0) corrosion already takes place, as this reaction leads to increased pH (Schmid et al 2015).

An increased presence of common anions results in increased sorption competition for As on the ZVI, which calls for higher dosage of the sorbent in order to maintain As removal efficiency in systems where this immobilization mechanism is significant. The inhibitory effect of HCO_3^- , CO_3^{2-} , and SO_4^{2-} is small, while for H_2PO_4^- , SiO_3^{2-} and PO_4^{3-} it is significant, the latter having the largest. The effect is more pronounced for As(V) than for As(III) and at higher pH due to the similarities between PO_4^{3-} and AsO_4^{3-} (arsenate ion) (Wang et al 2021).

2.2.3. Zero valent iron properties and modifications

Important ZVI particle properties for determining As removal efficiency are: availability of active sorption sites (Wang et al 2021), particle size, surface composition, extent of corrosion of the Fe(0) core and particle mobility (Schmid et al 2015).

Availability of active sorption sites can be enhanced by increasing the dose of ZVI or using nZVI rather than mZVI because of its inherent higher specific surface area (Wang et al 2021). On the other hand, the bare nZVI experience aggregation to a larger extent than mZVI due to the colloidal nature of the nano particles (Li et al 2006), which decreases its available surface area and therefore reduces efficiency. The colloidal nature of nZVI also hampers its mobility in the soil pores due to its increased size by aggregation and adhesion to soil particles (Sirk et al 2009). A field test has shown that the effect of this could restrict nZVI transport down to a few cm from the injection point (Li et al 2006). This colloidal instability has been successfully alleviated by adding different surface modifications to the

nZVI, such as sulfides, polymers or surfactants (Schmid et al 2015, Wu et al 2018). A possible drawback for using surface modified nZVI is reduced reactivity due to blocking of reactive sites (Phenrat et al 2009). Modifying nZVI with sulfide has shown to not only stabilize the particles in solution, but also adding removal mechanisms that are not present for pristine nZVI, which compensates for loss of removal efficiency in a way other surface modifications have failed to (Wu et al 2018).

Sulfidated ZVI

S-ZVI are ZVI particles that are synthesized along with or before addition of sulfur by compounds chosen by the producer (Fan et al 2017).

Unlike the smooth Fe(hydr)oxide surface of ZVI, the corrosion of S-ZVI develops an irregular shell of a mixture of Fe(hydr)oxide and FeS covering the Fe(0). Though occurring and similarities in the products formed, this corrosion is reduced as compared to bare ZVI due to its surface FeS. This gives the S-ZVI an advantage over ZVI in the form of increased life span (delayed depletion of the Fe(0) core) and comparably high reactivity towards As, even when comparing the sorbents after aging (Singh et al 2021). Increased S/Fe ratio of the ZVI increases the irregularity and thickness of the shell, which increases available sorption sites for As (Wu et al 2018).

The combined FeS and Fe(hydr)oxide shell of S-nZVI makes immobilization of As by S-nZVI more complex than that of nZVI (Wu et al 2018). Singh et al (2021) tested S-nZVI in anoxic conditions and found that the major removal mechanism for As(III) and As(V) with S-nZVI was through outer-sphere complexation, without initial reduction to lower valency species. Similarly to nZVI, S-nZVI has shown generally a more negatively charged surface in alkaline conditions and more positively charged in acidic conditions. Negatively charged As(V) aqueous species are thus adsorbed better in acidic pH and adsorption drastically declines at more alkaline pH values (Singh et al 2021). Furthermore, these authors observed immobilization of (mainly) As(III) by precipitation of As_2S_3 on the FeS surface (Singh et al 2021). Because the S-nZVI shell also contains Fe(hydr)oxides as regular nZVI does, the S-nZVI also offers some As immobilization by coprecipitation as Fe/As-hydroxides (as explained in section 2.2.1)(Singh et al 2021). Singh et al (2021) could not observe reduction of As(III) to lower valence As species.

Wu et al (2018) on the other hand suggested that inner-sphere complexation on the combined shell of the S-nZVI and coprecipitation of Fe/As/S-hydroxides were the main removal mechanisms for As(III). As(III) removal rate by S-nZVI was higher than that of regular nZVI in the pH range 3-9 (Wu et al 2018). They found that the removal capacity of S-nZVI was higher in oxic conditions than anoxic conditions. This was explained by dissolved O_2 favoring formation of Fe-S-H

groups and the subsequent adsorption of As to these. Additionally, most As(III) was oxidized to As(V) in aerobic conditions. In anaerobic conditions, only part of the As(III) was oxidized to As(V) (Wu et al 2018).

2.3. ICP-MS analysis of As

2.3.1. Working principle of ICP-MS

Inductively coupled plasma mass spectrometry (ICP-MS) is an analytical method that stands out by its comparably low detection limits. Constituent atoms of the sample injected to the instrument are ionized in the plasma, usually made up by argon (Ar). Upon reaching the mass analyzer, ions are distinguished by their mass-to-charge ratio (m/z^+). The then detected ion signals are converted into concentrations by initially having calibrated the instrument with signals that are detected when analyzing known concentrations of the element of interest (called calibration standards) (Wilschefski and Baxter 2019).

2.3.2. Internal standard

The ICP-MS technology is not without of flaws, it commonly experiences analyte signal amplification or suppression caused by drift in the instrument and matrix effects by the sample. A method to compensate for this is using internal standards. The internal standard is a solution of known concentration of an element, which is continuously injected to the instrument along with the analyte during analysis. The idea is that, by injecting the internal standard along with the analyte, any drift or matrix effects that will affect the analyte, will affect the internal standard element in a similar manner. This will allow measured shift from its prepared concentration to be transposed onto the measured concentration of the analyte (Wilschefski and Baxter 2019).

In order for the internal standard to be compatible with the analyte i.e., react similarly to drift and matrix effects, the basics of ICP-MS call for the two elements to have similar mass and first ionization energy. Additionally, the internal standard should neither cause nor experience spectroscopic interference upon junction with the sample (see section 2.3.3) (Wilschefski and Baxter 2019).

2.3.3. Interferences

ICP-MS interferences are analyte signal amplification or suppression, and are split up into spectroscopic and non-spectroscopic, with subcategories. Spectroscopic interferences are caused by non-analyte ions that have the same m/z^+ as the analyte, and non-spectroscopic interferences arise due to instrument drift and sample matrix characteristics. The manifestation of them is governed partly by the analyte, and As

suffers from the spectroscopic interference of polyatomic ions. Their formation is allowed by the heat in the plasma - their constituents stemming from sample matrix, the plasma Ar or other gases used for various purposes in the instrument. Chloride (Cl), which is common in natural waters and therefore introduced to the system by water sample analysis, forms $^{40}\text{Ar}^{35}\text{Cl}^+$ with Ar gas that is maintaining the plasma. This amplifies the signal at $m/z^+ 75$, interfering with the detection of $^{75}\text{As}^+$ (Wilschefski and Baxter 2019).

Methods to attenuate non-spectroscopic interferences in ICP-MS are not as successfully developed as the ones for spectroscopic interferences, though using an internal standard is one of them (see section 2.3.2) (Wilschefski and Baxter 2019). This section therefore focuses on spectroscopic interferences for As and the means to counteract them.

A way to mathematically correct for the $^{40}\text{Ar}^{35}\text{Cl}^+$ interference on the As signal at $m/z^+ 75$ is to relate the signal of the $^{40}\text{Ar}^{37}\text{Cl}^+$ (at $m/z^+ 77$) to $^{40}\text{Ar}^{35}\text{Cl}^+$, using the natural abundance ratio of the two Cl isotopes. The resulting correction equation can then fortify the $^{75}\text{As}^+$ signal by subtracting the contribution that the polyatomic interference makes to the signal at $m/z^+ 75$ (Wilschefski and Baxter 2019):

$$^{75}\text{As} = ^{75}\text{m} - 3.125 \times [(^{77}\text{m}) - 0.815(^{82}\text{m})] \quad (1)$$

, where ^{75}m , ^{77}m and ^{82}m are the intensities in counts per second (cps) of $m/z^+ 75$, 77 and 82 measured by the ICP-MS, 3.125 is the ratio of the natural abundance of the Cl isotopes at $m/z^+ 35$ and 37 , and 0.815 is the ratio of the natural abundance of the selenium (Se) isotopes at $m/z^+ 77$ and 82 . The Se isotopes are taken into account to correct for the ^{77}Se interference on the $^{40}\text{Ar}^{37}\text{Cl}^+$ signal (Colon et al 2009). A similar correction is added in the equation below:

$$^{75}\text{As} = ^{75}\text{m} - 3.125 \times [(^{77}\text{m}) - 0.815(^{82}\text{m}) + 0.883(^{83}\text{m})] \quad (2)$$

, where eq. (1) is extended with correction for the intensity (cps) contribution of krypton (Kr) on $m/z^+ 82$. This extension is applied in case the Ar used in the instrument contains ^{82}Kr as an impurity, which calls for correction of ^{82}Se (U.S. EPA 1996, Colon et al 2009).

Another approach to curb spectrometric interferences is introducing a gas to the system, targeting the interfering ions by either chemical reactions or reduced kinetic energy upon collisions with the gas (Wilschefski and Baxter 2019). In the former case, a reactive gas is added, for example O_2 , which readily will form $^{91}\text{AsO}^+$ with As if it is present. This allows detection of As at the signal of $m/z^+ 91$ instead, and will therefore not be interfered by the species mentioned above (Neubauer 2010).

Kinetic energy discrimination (KED) involves injecting the system with an inert gas, for example helium (He). The primary effect it will have is physical: upon each

collision between the He molecules and the present ions, these will lose their kinetic energy. $^{75}\text{As}^+$ as analyte will be subjected to the same effect, though to a lower degree than the interfering polyatomic ions, because these will experience more collisions due to their larger cross-sectional area. This leads to the interfering ions not having enough energy to pass through the barriers that exist at borders within the system leading towards the detector, hence allowing the As be the sole contributor (ideally) to the signal at $m/z^+ 75$ (Wilschefski and Baxter 2019).

2.4. Column and batch testing

Laboratory scale investigation of various aspects of contaminated soils, for example contaminant solubility and leaching, is made possible by different types of system-setups. There is no technique to alone paint the full representation of field conditions, but different approaches are rather complementing of each other. Two of these options are batch testing which is used to investigate formation of a dynamic equilibrium of the system whereas column testing is used to investigate chemical equilibrium. Dynamic equilibrium is found exclusively in closed systems and explain the state at which the ratio of reactants and products remain constant, while backward and forward reactions are still ongoing and at the same rate. Chemical equilibrium is the state when the concentrations of reactants and products remain constant, hence the reactions have come to a halt.

In batch tests, environmental systems are built by adding aqueous solution and other relevant constituents to a container. This container is sealed with headspace and then shaken during a determined timeframe before the solid and/or liquid phases are sampled and analyzed for parameters of interest (Andreottola et al 1997). Environmental systems are in column tests stacked without headspace, and solutions are then injected for a determined timeframe. There is simultaneous and constant outflow from one or several outlets of the column (Gratwohl and Susset 2009).

2.4.1. Comparison column and batch tests

In column leaching tests, the constant extraction during the experiment timeframe decreases the concentration of some of the system constituents that are present initially (Gratwohl and Susset 2009). This means that the total As content (A_{TOT}) of a column system will decrease with time. This results in an investigation of a less saturated system in terms of As. A natural consequence of this is that the As leaching from the open column system will gradually decrease over time until transitioning to steady state (Kalbe et al 2007). In contrast to this, in an As batch experiment, the same As saturation of the system will remain throughout its duration.

In batch tests, the entire system is usually allowed to reach equilibrium, while for column tests, only localized equilibria can be considered to control the mobilization because of the method's inherent loss of chemical reaction reactants and products from the open system (Lopez Meza et al 2008). Column tests are, however, more realistic than batch tests because the in-field subsurface is also an open system (Andreottola et al 1997).

Secondly, because of the shaking and therefore full dispersion of system particles in the solute of a batch setup, a large part of the adsorptive capacity of the system particles is made available for immobilization of dissolved As-species. This might lead to overestimation of the immobilizing capacity of the system in the field if the conditions favor sorption rather than desorption (Yong et al 1992 see Tanchuling et al 2005). Conversely, some studies have concluded that long-term batch underestimate adsorption (Gratwohl and Susset 2009, Löv et al 2019). This could be attributed to the shaking action, causing increased colloidal mobilization (Löv et al 2019). In a column system, where the solids are packed and fixed in space, there is much more particle-to-particle contact, making some adsorptive surfaces inaccessible (Yong et al 1992 see Tanchuling et al 2005). This better reflects the amount of solid-liquid contact surfaces in field conditions, where particles are in contact and not flushed around in the soil solution to a significant degree.

Before batch test samples can be analyzed, the solid and liquid phase are usually separated, and this can be performed with various techniques. The choice of the solid/liquid separation technique influences the results in the subsequent analysis, making batch test results operationally defined. Column test samples can be analyzed without this pre-analysis treatment, hence possibly giving more reliable results (Susset and Leuchs 2008 see Gratwohl and Susset 2009).

The concept of liquid to solid ratio (L/S) differs somewhat between batch and column systems in the sense that for the former it is the ratio of added liquid to added solid. The L/S is thus set in batch tests once the experiment is initiated. In column experiments, L/S is also the amount of liquid that has been in contact with the solid phase, but the L/S obviously increases as the experiment progresses, due to the continuous flow of eluent and eluate.

Column tests represent field conditions better by keeping the soil fixed in place and allowing the advective transport of possible dissolved species through the simulated subsurface by a chosen flow velocity (Kalbe et al 2007, Andreottola et al 1997, Lopez Meza et al 2008). If there are kinetic constraints in chemical reactions of interest, the constant through-flow might help predict what is actually leached because of the limited contact time between solids and the liquid (Krüger et al 2012, Naka et al 2016). Batch tests might have difficulties representing this because of the constant contact between the same solid and liquid pools and maximized contact surfaces due to continuous mixing (Gratwohl and Susset 2009). Experiment

duration can be shortened at the possible expense of not reaching equilibrium, but the constant mixing of the constituents is still not representative for field conditions.

Batch tests are a relatively simple and fast method of investigating a system and provide an opportunity to observe possible mechanisms that are the first determinators of a species being mobile or not. Batch tests also allow studying the kinetics of these mechanisms. However, batch tests do not offer insight to the transport-leaching aspect of a contaminated site because of the closed system and shaking which is not representative for the physical movement in the field (Krüger et al 2012, Andreottola et al 1997). The column tests are thus more dynamic systems predicting the mechanisms between solid and liquid phases in interplay with transport of the liquid and soluble constituents through the subsurface (Kalbe et al 2007, Andreottola et al 1997). Indeed, column tests have shown to better predict long-term field conditions than batch tests (Lopes Meza et al 2008).

However, both methods might have a weakness in terms of connectivity to field conditions due to the treatment of soil samples in preparation of experiments: the homogenizing, sieving and drying might modify pH and ionic strength of eluate, redox potential, cation exchange capacity and soil specific surface area, which all control metal(loid) solubility (Löv et al 2019). This should be kept in mind, particularly when using these tests as precursor to pilot and field-scale operations.

2.4.2. Preliminary studies of Hjärtevad - batch tests

Batch tests using aquifer sediment samples from Hjärtevad have previously been performed, studying the leaching of As with and without sorbents (nZVI, S-nZVI, mZVI and S-mZVI) in solution prepared to mimic the average ionic composition in the field (artificial groundwater, AGW) (Yet to be published, Thiago Formentini). The test was performed for 23-30 days. Every sampling in Figure 2 is from a different batch replicate, hence showing the conditions after given contact times between the solid and solution.

Results show that the batch system without sorbent, i.e. containing exclusively contaminated sediment and AGW, experienced a sharp increase in mobilization of total As (A_{STOT}) from 0 to 2 days contact time, but remained relatively unchanged until 10 days (Figure 2). When contact time was extended to 15 days, the mobilization more than doubled, and the increase to 17 days contact time indicated a relatively high increase in mobilization rate. Mobilization continued increasing with contact time up to 30 days. The As(III) concentration in solution in proportion to the A_{STOT} concentration increased when contact time was extended to 15 days. The contact time after which As mobilization was at its highest, the As(III) made up roughly 100% of A_{STOT} . The increased A_{STOT} concentration in the solution could for the most part be ascribed to mobilization of As(III), which as explained earlier, is considered the more mobile form of As. pH and redox potential (Eh) remained

relatively stable throughout the experiment at pH around 7 and +50 mV, respectively.

For the batches with S-mZVI, A_{TOT} immobilization sharply increased, with concentration dropping from roughly $100 \mu\text{g L}^{-1}$ to $50 \mu\text{g L}^{-1}$ when extending contact time from 0 to 2 days. A_{TOT} in solution remained around this level up to 30 days, with a final concentration of $29 \mu\text{g L}^{-1}$. As compared to the control batches, S-mZVI contributed to immobilization of As, as soluble A_{TOT} was as high as $100 \mu\text{g L}^{-1}$ and for the control around $800 \mu\text{g L}^{-1}$. The As speciation in the solution was mainly As(V), which stands in contrast to the control batches where a large part of As in solution was As(III). S-mZVI promoted immobilization and/or oxidation of As(III). pH and Eh remained relatively stable around 7.5 and -100 mV respectively, as compared to pH 7 and +50 mV for the control batches.

For the S-nZVI batches, A_{TOT} in solution remained relatively stable irrespective of contact time. The As speciation in solution was mainly As(V). As compared to the control batches, S-nZVI contributed to immobilization of As, as mobilized A_{TOT} was kept around $100 \mu\text{g L}^{-1}$, maximum $150 \mu\text{g L}^{-1}$. Hence, the performance was not as good as for S-mZVI. As(III) was immobilized and/or oxidized by S-nZVI. pH increased with contact time, from 8 to 9.5, hence higher than for the control batches. Eh shifted after half of the contact time tested, from a plateau of -100 to -200 mV. Generally, Eh was much lower than for the control batches.

In the mZVI batches, As was completely immobilized irrespective of contact time, and the A_{TOT} concentration at day 30 was only $11 \mu\text{g L}^{-1}$. pH increased with contact time from 8 to 10, hence higher than for the control batches. Eh fluctuated around -150 to -250 mV in the most contact times, but with a drop to -300 and -350 after a contact time > 25 days. Generally, Eh was much lower than for the control batches.

In the nZVI batches, As was completely immobilized, irrespective of contact time, and the A_{TOT} concentration at day 23 was only $19 \mu\text{g L}^{-1}$. pH increased from 8 to 9.5 with contact time up to 15 days. Eh increased with contact time to 12 days, then dropped dramatically with contact time of 15 days. Generally, Eh was lower than in the control batches.

In summary, the batch tests indicated that all tested sorbents have the potential to immobilize As in the Hjältevad soil and groundwater. Though, the non-sulfidated ZVI performed faster in the conditions and time frame tested, and lower As concentrations remained in these batch solutions as compared to the sulfidated ZVI-batches.

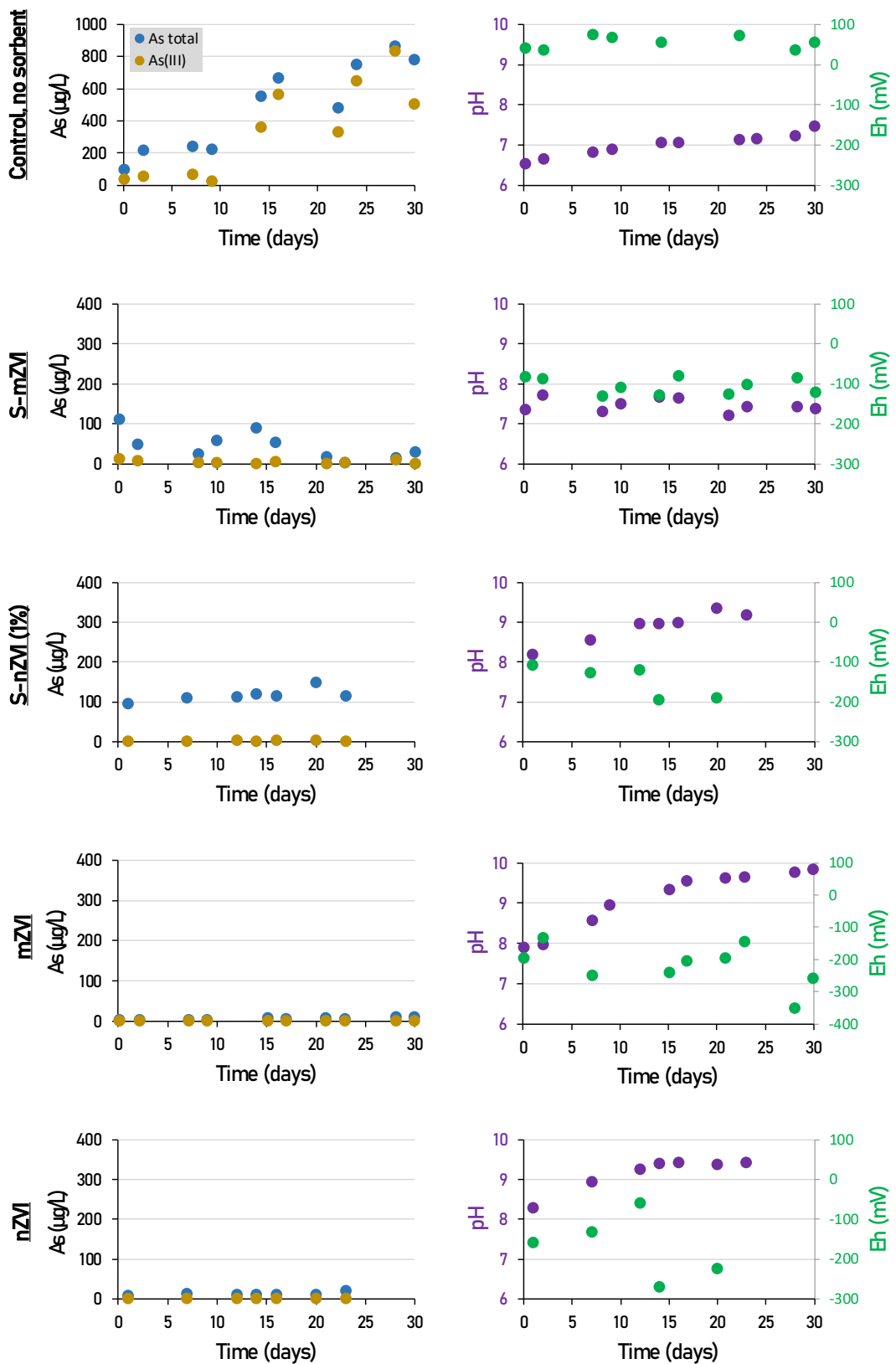


Figure 2. Results from up to 30 days batch tests. As_{TOT} and $As(III)$ concentrations in solution shown in $\mu\text{g L}^{-1}$ to the left. Note the scale difference of the y-axis for the batch system without sorbent. Eh shown mV and pH values for respective batch systems to the right.

3. Material & methods

3.1. Site description

The sediment used in the column experiments was sampled at an As-contaminated site in Hjärtevad, Eksjö municipality, Jönköping County in Sweden. This is a site where wood impregnation, using mainly chromated copper arsenate (CCA), was performed the years 1949-1985 (Figure 3) (SWECO 2019).



Figure 3. The area of the former impregnation plant in Hjärtevad. Also shown is the position of the former storage tank of the impregnation solution, deep shaft and sampling points for sediment and ground water. Standardkartan © [OpenStreetMap contributors](#), licensed under [CC BY-SA 2.0](#).

The area of the former wood impregnation plant is approximately 5.3 ha and the soil consist of glacial sediments in a layer of 40 m overlying the granite bedrock. The texture of the sediment becomes less coarse with depth, from gravel, sand to silt, but the texture is dominated by sand regardless of depth. Hydraulic conductivity thus also decreases with depth and exhibits a wide range (10^{-5} - 10^{-3} m s^{-1}). The groundwater drains out of the area in a NW direction (17.0°) with an average hydraulic gradient of 0.16 % (SWECO 2019).

Leakage from an impregnant-storage tank was discovered 1968 at the site. Upon discovery of the leakage, sampling wells were installed to monitor the contamination, and concentrations up to 2500 mg L⁻¹ As were found in the groundwater near the source. It was initially estimated that 65-80 kg As was released from the tank, but later estimations say that 2000-3000 kg of As is the total amount that has been released. Also contributing to the contamination was dripping from the treated products kept in the area (SWECO 2019).

When the tank leak was discovered, extraction and *ex-situ* treatment of ca 1000 m³ of contaminated groundwater was performed, though extracted at a much lower rate than the overall groundwater flow and at a shallow depth of the aquifer. The groundwater was further treated during 1984-1995 through aeration and re-filtration. In 1997, excavation and washing of the soil was performed, resulting in the removal of 4600 kg of As from the site. Then followed a period of monitoring the concentrations of contaminants, which was able to show a yearly increasing trend of dissolved As in the groundwater despite measures taken (SWECO 2019).

Sampling performed during 2016-2018 in 34 wells around the contamination zone amounted to 185 samples of which 30% exceeded the 10 µg L⁻¹ threshold for drinking water. In 2018, the As concentration in one of the monitoring wells downstream the major contamination zone reached 500 µg L⁻¹, i.e. 100 times the national guideline value for groundwater. The dominating speciation in the aquifer was found to be As(III) (78-100% in six wells), and in the most contaminated part, the groundwater concentrations were as high as > 2000 µg L⁻¹. It is believed that the efforts during 1984-1995 were based on miscalculations of the timing for the tank leak and spread of the contaminant plume, therefore not targeting a large enough area. Furthermore, the 1997 excavation left behind ca 1 ton As in the aquifer. In estimations for the future spread of the contamination after excavation, K_d values for the soil in the aquifer were estimated from leaching tests of irrelevant soil samples. The used K_d value was later found to be higher than the actual value found via leaching tests, and for that reason, the spread of the contamination plume was underestimated. The contaminant plume has migrated more than 225 m from the main source of contamination, which is the former storage tank for the solution (SWECO 2019).

The redox potential in the aquifer today is positive in the upper layer (>+ 50 mV) and decreases with depth to a values around -200 at +152 RH 2000 depth. pH is between 5 and 7 in the upper aquifer layer and increasing to values between 7 and 8 at +152 RH 2000 depth. Figure 4 depicts a stability diagram for As along with measured redox-potentials and pH of the ground water measured at the site the years 2016-2018 by SWECO. The measurements suggest that the prevalent species of As present in the aqueous phase of the aquifer is As(III) (SWECO 2019).

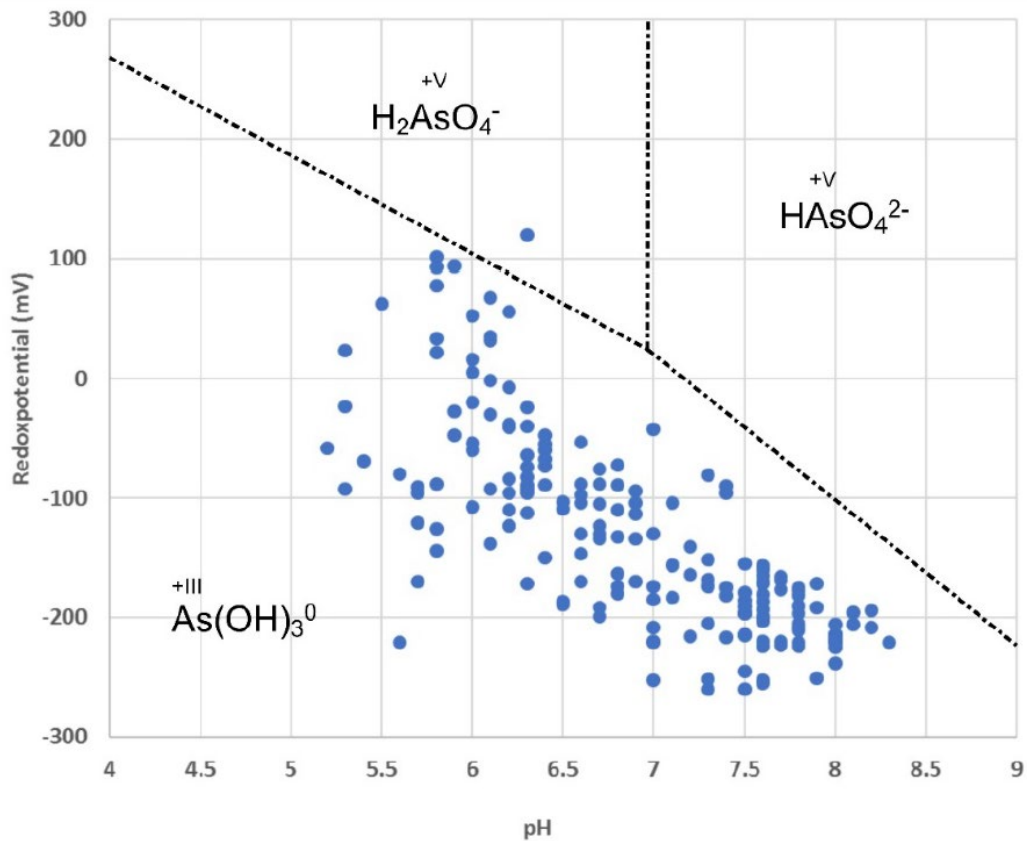


Figure 4. Stability diagram for As showing pH-redox-regions where As(III) and As(V) species are prevalent. Blue dots are measured pH and Eh in the soil at the site in Hjärtevad in the years 2016-2018 (SWECO 2019, p. 94).

Speciation of As performed in the field supported the hypothesis that As(III) dominates where redox potential is $<+ 50$ mV (SWECO 2019).

3.2. Sediment sampling

The sediment used for the column experiments was extracted at sample point 1904 during 2019 by SWECO (Figure 3). A core was taken at 16-18 m below the surface using a Sonic Geo Drill, with care taken to protect the sediment from exposure to O₂ during sampling and storage. This was ensured by applying pressurised water during sample transfer to keep O₂ from entering the system (so called “aqualock”) and separating the core from the piston by a gasket. The sample transfer was further O₂-proofed by enclosing the core in a closed PVC cylinder in the drilling hole while flushing it with gaseous nitrogen (N₂). The PVC cylinder with sample was transferred to an air-tight plastic bag and was within hours after collection frozen and stored in -20°C until further manipulation.

The sediment was later thawed in a glovebox before it was homogenized, split into subsamples in sealed aluminum foil bags (Mylar®), and again frozen and

stored in -20°C. For more details about the sampling procedures see Leicht (2021). Before initiation of column experiments, sediment was thawed and dried inside a glove box that is described further. Total As concentration in the sediment was determined to 46.9 mg kg⁻¹.

3.3. Method development ICP

Several methods for analyzing sub µg L⁻¹ concentrations of As in ICP-MS were investigated to find the optimal elimination of different polyatomic Cl⁻ interferences. The instrument used was a Perkin Elmer® NexION® 350D which offers several modes of analysis.

3.3.1. Standard mode

Artificial soil solutions with known concentrations of As and CaCl₂ were analyzed in standard mode (collision/reaction mode deactivated) without and with mathematical correction using eq. (1) and (2) (see section 2.3.3) to assess their ability to limit the interferences caused by CaCl₂ (⁴⁰Ar³⁵Cl⁺ and ⁴⁰Ca³⁵Cl⁺ at signal m/z⁺ 75). The artificial soil solutions were combinations of different concentrations of As and CaCl₂, corresponding to expected maximum concentrations in soil solutions: As 0, 1 and 10 µg L⁻¹, Ca 0, 0.2, 2, 20 and 200 µg L⁻¹ & Cl 0, 0.1, 1, 10 and 100 µg L⁻¹.

3.3.2. Collision mode with KED using He gas

The same artificial soil solutions as used in standard mode (see section 3.3.1.) were analyzed while introducing 5 mL min⁻¹ He gas into the collision/reaction cell.

3.3.3. Reaction mode using O₂ gas

The same artificial soil solutions as used in standard mode (see section 3.3.1) were analyzed while introducing 0.7 mL min⁻¹ O₂ gas into the reaction/collision cell. 20 blanks (2 % HNO₃) were analyzed to calculate the detection limit (LOD) and limit of quantification (LOQ) for this method.

3.4. Sorbents

A group of commercially available ZVI sorbents were used for the As retention experiments, each a potential candidate for future remediation of Hjältevad. Table 1 shows the technical specifications for each product. nZVI and S-nZVI are commercially available by the company NANO IRON, and are both delivered as

diluted suspensions of respective sorbents in water (14-18 wt% of Fe(0)) (NANO IRON 2016a, NANO IRON 2016b). The S-nZVI has a modification of a 0-1 % Fe(II) Sulfide coating (NANO IRON 2016b). Average sizes of the individual particles of both products are nominally 50 nm, though aggregation has been observed (Schmid et al 2015, Brumovský et al 2020, Brumovský et al 2021).

mZVI is commercially available by the company Hepure and is delivered as a solid powder of 95 % Fe(0). The average individual particle size is 44 μm (Hepure 2021). S-mZVI is commercially available from the company REGENESIS and is delivered as a viscous slurry of 30-50 wt% Fe(0) in glycerol, coated by 1-4 % Fe(II) Sulfide and contains also a proprietary dispersant. The individual particle size is < 5 μm (REGENESIS 2018).

Table 1. Characteristics of ZVI sorbents used in the column experiments.

Sorbent type	Commercial name	Producer	Nominal size	Nominal Fe(0) content (wt%)	Coating	State
nZVI	NANO FER 25S	NANO IRON	50 nm	14-18	none	Suspension
S-nZVI	NANO FER 25DS	NANO IRON	50 nm	14-18	Fe(II) Sulfide	Suspension
mZVI	Ferox Target	Hepure	44 μm	95	none	Powder
S-mZVI	S-MicroZVI®	REGENESIS	< 5 μm	30-50	Fe(II) Sulfide	Viscous slurry

Sorbent storage time from delivery to use differed. mZVI was stored for roughly two years and S-mZVI was stored for several months. nZVI and S-nZVI were freshly prepared by NANORION and used within a week after delivery. mZVI was stored in room temperature in a sealed plastic container, while nZVI, S-nZVI and S-mZVI were stored at +4°C until use.

3.5. Column experiments

This section describes the experimental setup used in this study to investigate the As retention performance/capacity of the four sorbents in the Hjältevad sediment. It is initiated with the general procedure of preparing a column before leading on to the preparation of the various compositions that were used in order to answer different questions, followed by the sampling procedures for the long-term experiment.

All procedures in this section were performed in a glove box. The glovebox was a Labconco®, Protector® Controlled Atmosphere Glove Box with controlled anoxic atmosphere, fed with purified N₂, and catalytic O₂ removal using AtmosPure® Re-Gen Gas Purifier. The O₂ concentration in the glove box was monitored continuously (Alpha Omega Series 3000 Trace Oxygen Analyser). This was below 15 mg L⁻¹ during manual operation and 3 mg L⁻¹ overnight. The anoxic atmosphere was imperative to mimic the redox conditions prevailing in the contaminated subsurface at Hjältevad (Figure 4).

3.5.1. Artificial groundwater

Artificial groundwater (AGW) was used during column wet packing as well as eluent during leaching. The AGW was prepared to match groundwater samples from Hjärtevad monitoring wells 1708_2 and 1709_2 (Figure 3), aiming to reflect their average ionic composition. Ultrapure water (ELGA PURELAB® ultra ionic) was degassed with pure N₂ for an hour, immediately transported into a glovebox, and added to a 5 L Erlenmeyer flask up to mark. Dissolved stocks of salts (Table 2) were added and concentrated hydrochloric acid (HCl) was added until pH 6 was achieved.

Table 2. Salts, their respective stock concentrations and amounts used for AGW preparation.

Salt	Target AGW composition		Preparation of individual stock solutions			Stock added to AGW
	Conc. (mmol L ⁻¹)	Conc. (mg L ⁻¹)	Stock conc. (mmol m L ⁻¹)	Mass weighed (g)	Diluted to (mL)	Volume of stock (mL) added to 5 L of AGW
K ₂ SO ₄	0.200	34.852	0.200	0.6970	20	5
CaCl ₂ ·2H ₂ O	0.450	66.157	0.450	1.3231	20	5
NaHCO ₃	0.750	63.005	0.750	1.2601	20	5
KHCO ₃	0.050	5.006	0.050	0.5006	100	5
MgCl ₂ ·6H ₂ O	0.100	20.330	0.100	0.4066	20	5
MnCl ₂ ·4H ₂ O	0.010	1.979	0.010	0.1979	100	5
NH ₄ Cl	0.015	0.802	0.015	0.8020	1000	5
KH ₂ PO ₄	0.001	0.136	0.001	0.1360	1000	5

3.5.2. Packing procedure and percolation

Diba Omnifit® EZ Chromatography Columns of borosilicate glass, dimensions $2,5 \times 10$ cm were used in the experiments. Bottom end-piece of each column was lined with a 70 μ m Nylon mesh filter (Spectrum® Laboratories, Inc.) after removal of the filter included by the manufacturer. The removal was done because the filters included with end-pieces have shown major effect on engineered nanomaterials (ENM) breakthrough curves in some cases (Norrfors et al 2021). The new filters were added in order to prevent clogging of column inlet and outlet by sediment or sorbents.

The column packing procedure was adapted from Norrfors et al (2021), aiming at producing water-saturated columns (Figure 5). The first step was adding approximately 2 mL of the chosen packing solution. This was ultrapure water containing sorbents in most cases (see sections 3.5.3, 3.5.4, 3.5.5 and 3.5.6 for respective composition details). Dry solid phase (i.e. sediment with or without sorbents) was added (see sections 3.5.3, 3.5.4, 3.5.5 and 3.5.6 for respective composition details). This sequence was then repeated until the column length

reached approximately 10 cm. For every sequence, mild tapping of the column was done to release trapped air.

Solid phase was transferred to the columns using a spatula after careful homogenization (using a deep digging motion). Before every pipetting of packing solution containing sorbents (depending on the treatment for the column), the container was shaken to ensure homogenous distribution of the sorbent. The containers with solid phase and packing solution were weighed before and after completed packing procedure, to allow calculation of total pore volume and bulk density of the column. The column was then closed and tightened, and the length was measured to acquire its total volume. The final length of the tightly sealed columns measured 10 +/- 0.5 cm.

The experiments were run injecting the column with their respective eluent in a bottom-up fashion. The eluent and eluate were delivered through Teflon and Tygon tubes using a peristaltic pump of model ISMATEC Labinett BVP.



Figure 5. Packing of columns. Photos taken by author.

3.5.3. Preparatory experiment: Sorbent retention – No system manipulation

The aim of this experiment was to assess the sorbent retention in the columns. It was important for the purpose of the column tests that sorbent losses were minimal. Two columns were prepared according to section 3.5.2, both with uncontaminated

sediment (from the site), out of which one was prepared with nZVI, and the other with S-nZVI. 4 pore volumes (PV) of AGW were injected to each column (Figure 6). Sampling resolution was 30 minutes. The raw eluate-samples were prepared (see section 3.6) for analysis of Fe_{TOT} .



Figure 6. Preparatory column-experiment inside glove box. Photo taken by author.

3.5.4. Preparatory experiment: Sorbent retention - Addition of NaCl

The aim of this experiment was to assess whether sorbent retention in columns would be enhanced by aggregation of sorbents caused by the increased ionic strength of the column/soil solution. Though not a priority, this experiment potentially also allowed characterizing hydrological properties of the columns. Modelling breakthrough of inert tracers such as NaCl is commonly done to acquire the effective porosity and dispersivity of the columns. A column was prepared according to section 3.5.2 with uncontaminated sediment from the site and S-nZVI. 4 PV of 50 mM NaCl were injected into the column before switching eluent to AGW. The first 4 h had a sample resolution of 30 min. After that period, one last sampling was performed 23h after initiating the experiment. The raw eluate-samples were prepared (see section 3.6) for analysis of Fe_{TOT} .

3.5.5. Preparatory experiment: Short term leaching

Raw eluate (see section 3.6) was analyzed for A_{STOT} to ensure that leached As concentrations would be above the LOD. Additionally, the knowledge of the required amount of packing solution and sediment for the 10 cm column was used to calculate the amount of commercial product of ZVI needed in the packing solutions in order to reach the target concentration for the long-term experiment columns (Table 3 and Table 4). A column was prepared according to section 3.5.2 with contaminated sediment and AGW and was pumped through in a bottom-up, saturated flow for 23 h. A sample resolution of 30 min was used.

3.5.6. Long-term experiment

A total of 10 columns were prepared according to section 3.5.2. These columns had five different compositions in duplicate, each type aiming to represent a different field scenario: a type for each of the four investigated sorbents and one reference (“present day”) containing no sorbent. All columns were packed with contaminated sediment from the site. The mode in which sorbents were added to the columns differed because of the different states the commercial products are delivered in (Table 1 and Table 3). nZVI, S-nZVI and S-mZVI were added to their respective column duplicates by the packing solution as they are delivered as suspensions or slurries (Table 3). These sorbent packing solutions were prepared with known amounts of respective sorbent and ultrapure water (Table 4). As mZVI is delivered as a dry powder, it was added to its column duplicates by initially mixing a known amount of sorbent into a known amount of contaminated sediment before packing (Table 3 and Table 4). The reference column was prepared with exclusively AGW as packing solution (Table 3).

Table 3. Content of columns and procedure for mixing in the sorbents.

Sorbent	Solid phase	Packing solution	Target column C_{Fe} (% w/w)
nZVI	Contaminated sediment	Ultrapure water + sorbent (Diluted sorbent solution)	0.2
S-nZVI			
S-mZVI			
mZVI	Contaminated sediment + sorbent	Ultrapure water	1
Reference	Contaminated sediment	AGW	

Table 4. Concentration of Fe in commercial ZVI, mass used for preparation of sorbent packing phase, and its final amount & Fe concentration.

Sorbent	C _{Fe} of commercial product (g Fe kg ⁻¹)	Mass of commercial product used (g)	Amount of sorbent packing phase prepared	C _{Fe} in packing phase
nZVI	200	2.24	50 mL	8.934 mg mL ⁻¹
S-nZVI	200	2.24	50 mL	8.934 mg mL ⁻¹
S-mZVI	400	1.12	50 mL	8.934 mg mL ⁻¹
mZVI	Pure Fe (95 %)	2	200 g	1 g 100 g ⁻¹

AGW prepared according to section 3.5.1 was transferred into a 10 L container and pumped according to section 3.5.2. The AGW percolated through each column (Figure 7 and Figure 8) for a consecutive 52 days with a flow rate of average 193 mL day⁻¹. The flow rate was chosen to correspond to 3.4 years in the field (contact time was approximately 20 times higher than at Hjärtevad). Eluate was collected in 1 L Nalgene bottles of PP, PE and HDPE covered with parafilm, one assigned to each individual column.

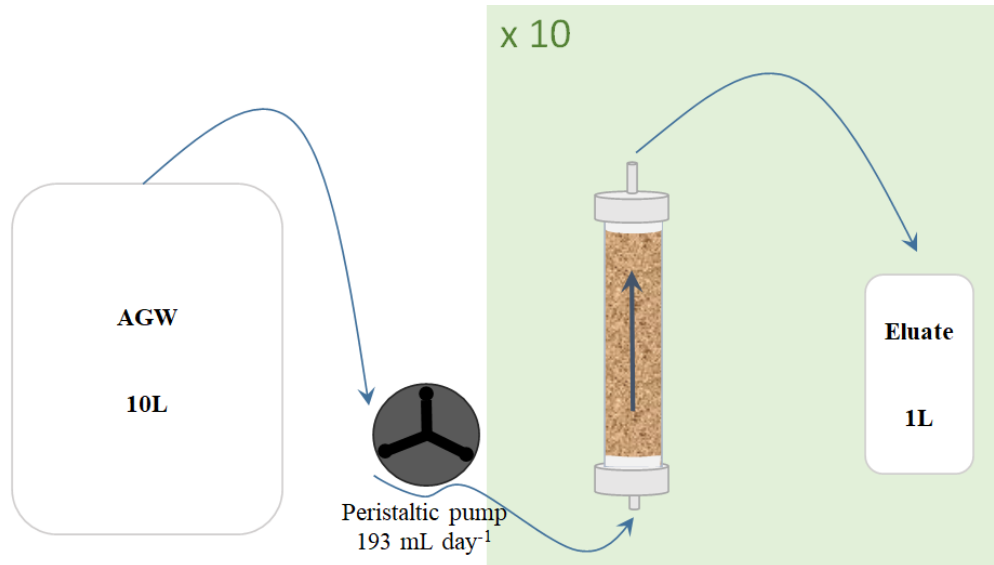


Figure 7. Long-term column experiment setup shown for one column. All 10 columns were simultaneously provided with AGW from the same eluent container with the same peristaltic pump. Eluate was collected in 10 separate containers.



Figure 8. Long-term experiment columns with their respective eluate containers inside the glove box. Shown in the foreground is the collective AGW container. Photo taken by the author.

Sample treatment

The eluates were sampled every 4th-5th day. Sampling consisted of weighing the eluate bottle to obtain the volume of eluates for the sample period, homogenizing and distributing into smaller containers for analysis and preparation (Figure 9): A_{STOT} and F_{TOT} were measured after digestion of the raw eluate (see section 3.6). The redox potential (Eh) (using an Orion™ Metallic Combination Electrode) and pH (using an Orion™ 8102BNUWP ROSS Ultra™ glass Electrode) were analyzed immediately in the raw eluate. The $< 0.45 \mu\text{m}$ fraction was separated using a membrane filter (Pall Acrodisc) to quantify the concentration of truly dissolved and colloidal (defined as $> 0.45 \mu\text{m}$) forms of As & Fe by comparing these concentrations with A_{STOT} and F_{TOT} , respectively. A sub-sample of the filtered eluate was passed through a cartridge (As speciation cartridge from MetalSoft Center) that selectively binds As(V). Comparing the non-retained As concentration with truly dissolved (i.e. non-colloidal) As then allows to quantify the As(III)/As(V) ratio of dissolved As. Membrane filtered and As-cartridge filtered samples were acidified to 1 % with analytical grade 65 % HNO_3 , sealed and stored at $+4^\circ\text{C}$.

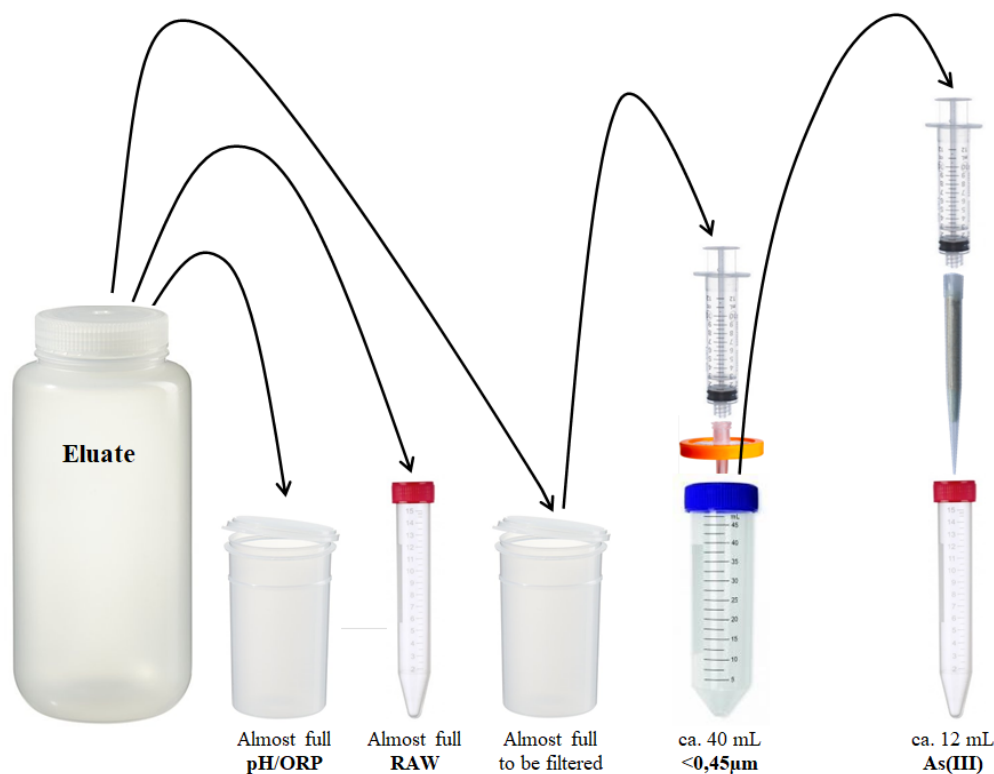


Figure 9. Sampling flow chart for long-term column experiment.

3.6. Microwave-assisted digestion

2 mL of raw eluate from each column was added to 6 mL of 7 M HNO₃ prepared from analytical grade 65 % HNO₃ in Teflon (Milestone) digestion tubes. All samples were digested in duplicate and blank samples (2 mL of ultrapure water + 7 M HNO₃) were added, yielding 22 digested samples per sample time point. The tubes were placed in a Milestone Ethos® Easy. The samples were heated at maximum power (1400 W) for 15 minutes following by 30 minutes at 1000 W, thus following the us epa 3051a standard procedure for analyzing soil samples (U.S. EPA 2007). After cooling, samples were transferred quantitatively to 50 mL-centrifuge tubes using ultrapure water. All samples were diluted to a final volume of 50 mL, sealed, shaken and stored at +4°C before ICP-MS analysis.

3.7. Elemental Analysis

Analysis was performed with ICP-MS in a Perkin Elmer NexION 350D. As_{TOT} and Fe_{TOT} concentrations in microwave-digested raw samples as well as the < 0.45 µm- and As(III)- fraction were analyzed using the respectively optimized method.

Elemental standards were prepared in the sample matrix (7 M HNO₃ or 1 % HNO₃) to ensure accurate calibration.

Due to technical issues with the in-house instrument, the optimized method was only used to analyze the long-term experiment samples up to the fourth sampling. Analysis of samples after the fourth sampling was performed by ALS Scandinavia AB with an ICP-MS.

4. Results

4.1. ICP-MS method optimization

Standard mode with and without correction equations overestimated As concentration, and the overestimation increased with increasing CaCl_2 concentration. The highest overestimations were with As concentration of $1 \mu\text{g L}^{-1}$.

Collision mode using He gas and reaction mode using O_2 gas showed similar sensitivity in As analysis, but upon recommendation by the in-house technician, reaction mode using O_2 gas was chosen.

LOD for As with the reaction mode using O_2 gas was determined to 0.013 ppb and LOQ to 0.038. ^{82}Se was used as internal standard. Iron concentrations in were analyzed with standard mode for low concentrations of iron and ^{115}In as internal standard.

4.2. Column protocol development

Fe-analysis showed that sorbent retention in the columns was not affected by adding NaCl to the system. There was no observable breakthrough curve produced upon a pulse-addition of NaCl.

As concentrations leaching from column with contaminated sediment and AGW were above LOD of the optimized ICP-MS method.

4.3. Long-term column leaching

Column duplicates generally showed low variation in measured eluate As and Fe concentrations, pH and Eh.

4.3.1. Iron

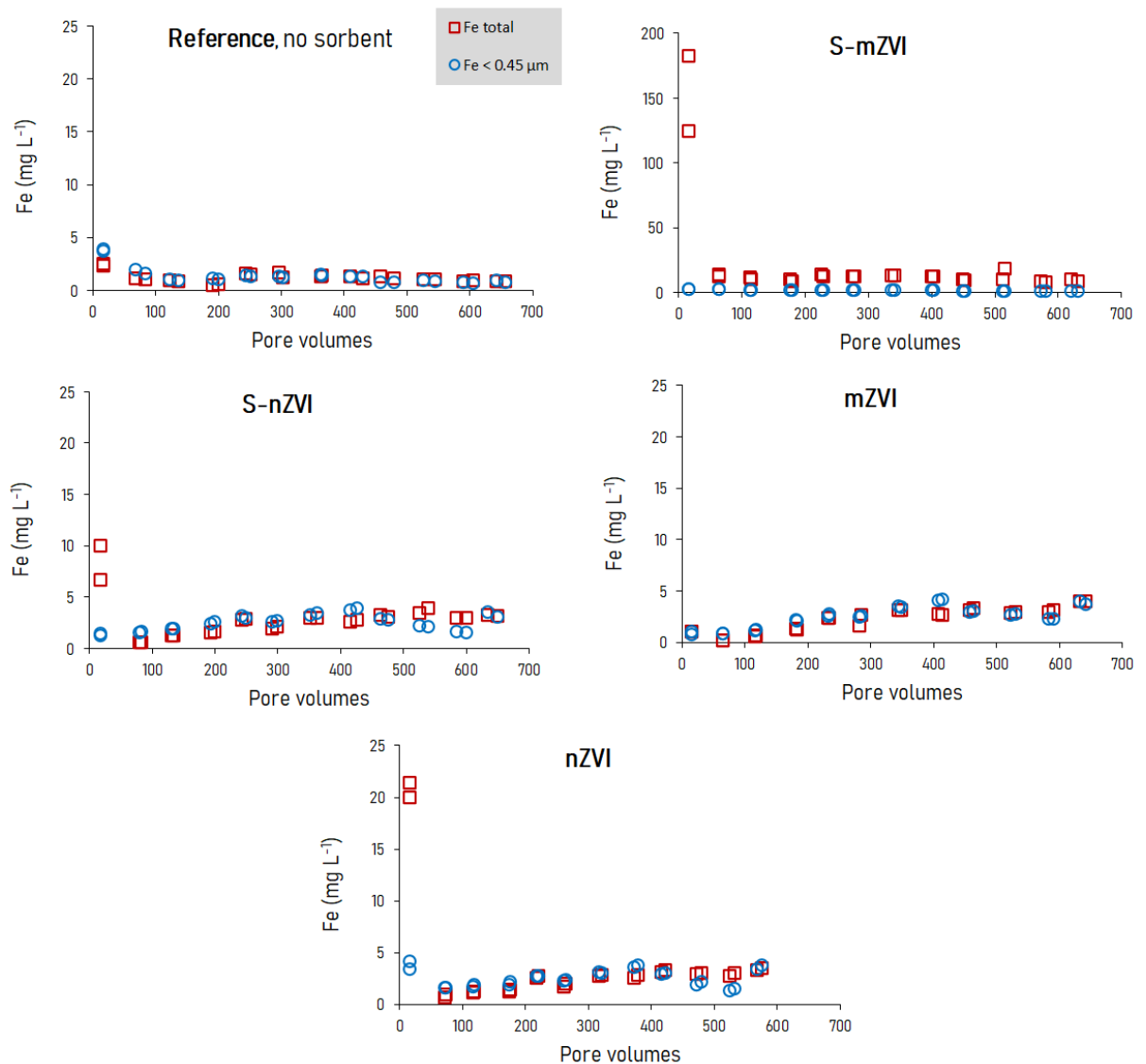


Figure 10. Fe leaching per respective column type in mg L⁻¹. Fe_{TOT} from respective duplicate shown in red squares and < 0.45 μm fraction from respective duplicate shown in blue circles. Time of experiment duration is expressed in number of pore volumes passed through respective column type.

The concentration of leached Fe_{TOT} in the eluate from the reference column duplicates decreased from the first sampling occasion to the second from approximately 2000 μg L⁻¹ to approximately 1000 μg L⁻¹ (Figure 10). After the second sampling occasion, the leached Fe_{TOT} concentration remained constant for each sampling period throughout the experiment. The concentration of leached Fe in the < 0.45 μm fraction (truly dissolved + colloidal) followed the same trend.

Note the difference in scale of y-axis for the figure for the S-mZVI column duplicates as compared to other Fe-leaching figures (Figure 10). The concentration of leached Fe_{TOT} in the eluate from the S-mZVI duplicates decreased very sharply from the first sampling occasion to the second from average (of the column

duplicates) 153 500 $\mu\text{g L}^{-1}$ to average 13 300 $\mu\text{g L}^{-1}$, but the concentration differed between the column duplicates noticeably the first sampling occasion. From the second sampling occasion to the end of the experiment, the leached Fe_{TOT} concentration remained relatively stable. The concentration of leached Fe in the $< 0.45 \mu\text{m}$ fraction (truly dissolved + colloidal) remained stable throughout the entire experiment, though at slightly higher levels from the first to the second sampling occasion. The higher being at average 2 500 $\mu\text{g L}^{-1}$ and the lower concentrations around 1 300 $\mu\text{g L}^{-1}$. By the first sampling, the leached Fe_{TOT} concentration was much higher than that of Fe in the $< 0.45 \mu\text{m}$ fraction.

The concentration of leached Fe_{TOT} in the eluate from the S-nZVI duplicates decreased sharply from the first sampling occasion to the second from average (of the column duplicates) 8 300 $\mu\text{g L}^{-1}$ to average 600 $\mu\text{g L}^{-1}$ (Figure 10). From the third sampling occasion to the end of the experiment, there was a slightly increasing trend in leached Fe_{TOT} concentration though with some fluctuation. The leached Fe_{TOT} concentration was average 3 200 $\mu\text{g L}^{-1}$ at the last (12th) sampling occasion. By the first sampling, the leached Fe_{TOT} concentration was noticeably higher than that of Fe in the $< 0.45 \mu\text{m}$ fraction (truly dissolved + colloidal). The concentration of leached Fe in the $< 0.45 \mu\text{m}$ fraction was average (of the column duplicates) 1 300 $\mu\text{g L}^{-1}$ at the first sampling occasion, from which it showed a slightly increasing trend to the eighth sampling occasion where leached average concentration was 3 900 $\mu\text{g L}^{-1}$. From the ninth sampling occasion there was a decreasing trend to the 11th, to average 1 600 $\mu\text{g L}^{-1}$. The leached concentration increased again to the last and 12th sampling occasion, with an average of 3 300 $\mu\text{g L}^{-1}$.

The concentration of leached Fe_{TOT} in the eluate from the mZVI duplicates decreased from the first sampling occasion to the second from 1 034 $\mu\text{g L}^{-1}$ to average 195 $\mu\text{g L}^{-1}$ (Figure 10). From the third sampling occasion to the end of the experiment, there was an increasing trend in leached Fe_{TOT} concentration though with some fluctuation. The leached Fe_{TOT} concentration was average 4 000 $\mu\text{g L}^{-1}$ at the last (12th) sampling occasion. The concentration of leached Fe in the $< 0.45 \mu\text{m}$ fraction (truly dissolved + colloidal) was average (of the column duplicates) 921 $\mu\text{g L}^{-1}$ at the first sampling occasion, from which it showed a slightly increasing trend to the eighth sampling occasion where leached average concentration was 4 100 $\mu\text{g L}^{-1}$. From the ninth sampling occasion there was a decreasing trend to the 11th, to average 2 300 $\mu\text{g L}^{-1}$. The leached concentration increased again to the last and 12th sampling occasion, with an average of 3 900 $\mu\text{g L}^{-1}$.

The concentration of leached Fe_{TOT} in the eluate from the nZVI duplicates decreased very sharply from the first sampling occasion to the second from average (of the column duplicates) 20 100 $\mu\text{g L}^{-1}$ to average 800 $\mu\text{g L}^{-1}$ (Figure 10). From the third sampling occasion to the end of the experiment, there was a slightly increasing trend in leached Fe_{TOT} concentration though with some fluctuation. The leached Fe_{TOT} concentration was average 3 400 $\mu\text{g L}^{-1}$ at the last (12th) sampling

occasion. By the first sampling, the leached Fe_{TOT} concentration was much higher than that of Fe in the $< 0.45 \mu\text{m}$ fraction (truly dissolved + colloidal). The concentration of leached Fe in the $< 0.45 \mu\text{m}$ fraction in the eluate decreased from the first sampling occasion to the second from average (of the column duplicates) $3\,800 \mu\text{g L}^{-1}$ to average $1\,600 \mu\text{g L}^{-1}$. From the third sampling occasion, the leached Fe in the $< 0.45 \mu\text{m}$ fraction showed a slightly increasing trend to the eighth sampling occasion where leached average concentration was $3\,700 \mu\text{g L}^{-1}$. From the ninth sampling occasion there was a decreasing trend to the 11th, to average $1\,400 \mu\text{g L}^{-1}$. The leached concentration increased again to the last and 12th sampling occasion, with an average of $3\,600 \mu\text{g L}^{-1}$.

Fe leaching as compared to reference column

Fe leaching from the S-mZVI duplicates was much higher than from the reference column, especially by the first sampling, when the leached concentration was roughly 77 times higher than that from the reference duplicates, dominantly of the $> 0.45 \mu\text{m}$ fraction.

Fe leaching from the S-nZVI duplicates was roughly twice as high as the leaching from the reference duplicates after the third sampling, with slight increase with time. However, the first sampling, it was about four times higher, dominated by the particulate fraction.

The Fe leaching from the mZVI duplicates was lower than that from the reference duplicates from the first to the third sampling. By the fourth sampling onward, the Fe leaching from the mZVI duplicates exceeded the one from the reference duplicates with continuous increase (similar to S-nZVI), at the last sampling reaching four times higher leached concentration.

The Fe leaching from the nZVI duplicates was very similar to that from S-nZVI, with a higher leaching by the first sampling. There, the leached Fe concentration was about 10 times higher than that from the reference duplicates and majorly made up of the particulate fraction.

Mass balance

The total amount of leached Fe_{TOT} for the entire long-term experiment was the largest for the S-mZVI duplicate columns, with an average $136\,161 \mu\text{g}$, corresponding to 16 % of the initial input by the sediment and sorbent (Table 5). The second and third largest Fe_{TOT} leaching was found for the nZVI and S-nZVI duplicate columns at around $23\,300 \mu\text{g}$, corresponding to around 3 % of the initial input by the sediment and sorbent. The mZVI duplicates leached on average $19\,126 \mu\text{g}$, 1.2 % of the initial input by sediment and sorbent. The reference duplicates leached average $9\,808 \mu\text{g}$, 1.4 % of the initial input by the sediment.

The Fe_{TOT} leached from the duplicates were 100% made up of their $< 0.45 \mu\text{m}$ fraction except for the S-mZVI, for which this share was 11 %.

Relating the Fe_{TOT} losses from the treated duplicates to the losses from the non-treated duplicates (reference), i.e the excess leaching in % of Fe added by the respective sorbents, the shares were in falling order: S-mZVI >> S-nZVI > nZVI > mZVI.

Table 5. Mass balance for leached Fe for the entire experiment duration for each column type.

Column	Mass balance Fe leached				
	Fer _{OT}			Fe < 0.45 μm	
	(μg)	(% of input by sediment and sorbent)	Excess leaching compared to reference (% of Fe _{ZVI} added)	(μg)	(% of Fe _{OT} leached)
nZVI	23388	2.6	9	23985	100
S-nZVI	23285	3	10	25410	100
Reference	9808	1.4	--	11345	100
mZVI	19126	1.2	1	24940	100
S-mZVI	136161	16	93	14346	11

4.3.2. pH and Redox Potential (Eh)

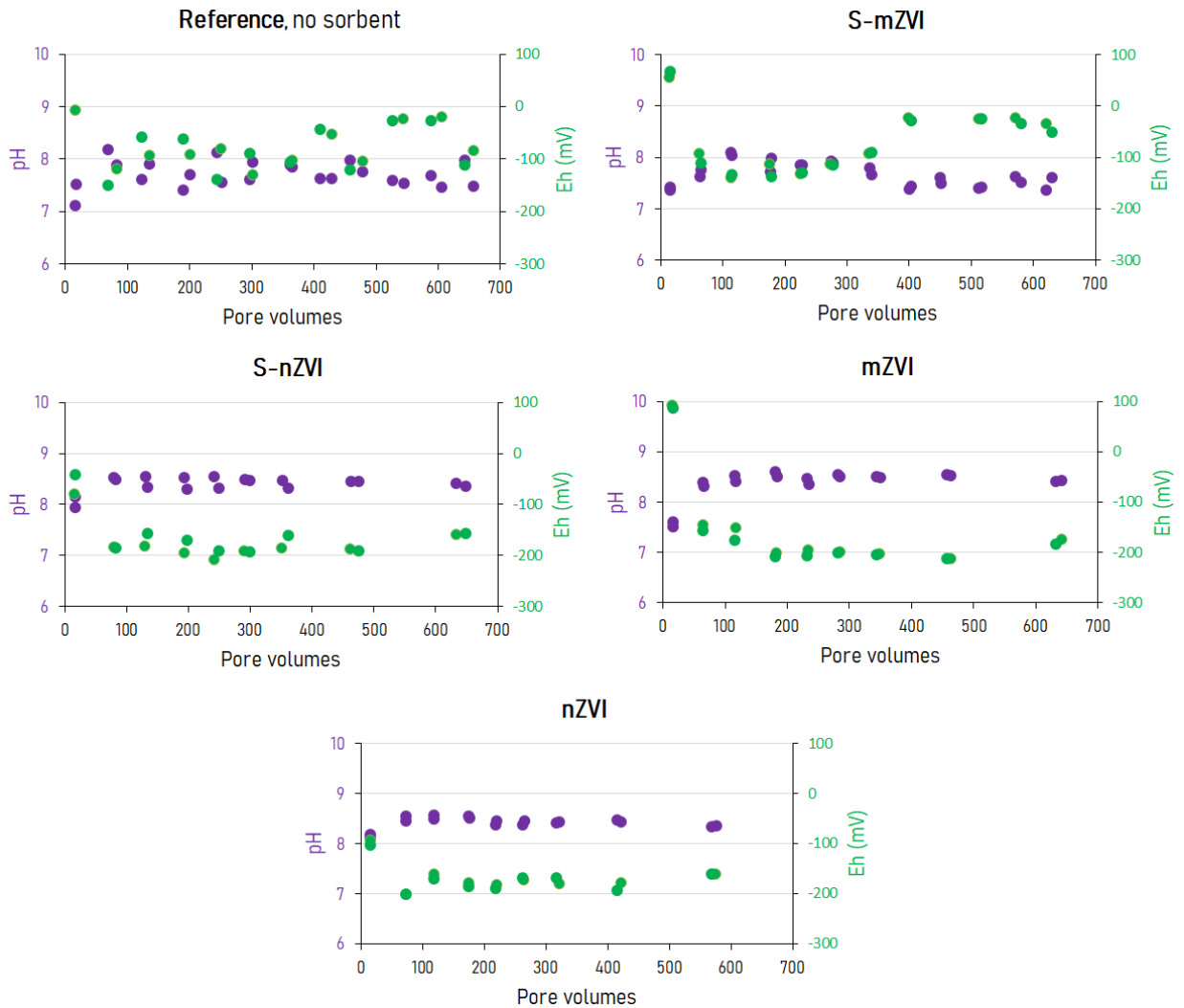


Figure 11. pH (purple and left y-axis) and Eh in mV (green and right y-axis) measured in eluates from respective column type. Time of experiment duration is expressed in number of pore volumes passed through respective column type.

The pH in the eluate from the reference duplicates was stable with an average of 7.7 throughout the experiment (Figure 11). The Eh in the eluate fluctuated around -70 mV \pm 80 mV (highest value -7 and lowest -149) with an average of -72 mV (of column duplicates for all sampling occasions).

By the first sampling occasion, the pH in the eluate from the S-mZVI duplicates was around 7.4, and increased to the third sampling occasion to pH 8 (Figure 11). The pH was stable around 8 until sampling occasion six. From the seventh sampling occasion (340 PV) pH shifted to lower values, being stable at around 7.5 from sampling eight towards the end of the experiment. By the first sampling occasion, the Eh in the eluate was positive, at an average of +61 mV (of the column duplicates). There was a sharp drop to the second sampling occasion, to an average

of -103 mV. The Eh values decreased slightly more to sampling occasion three, before a very slight increase initiated until the seventh sampling occasion where Eh was -92 mV on average. By the eighth sampling occasion (403 PV), Eh sharply shifted to higher values, and was stable at around -30 mV to the end of the experiment.

The first sampling occasion, the pH in the eluate from the S-nZVI duplicates was average 8.1 (of the column duplicates), and increased to the second sampling occasion to average 8.5 around where it remained stable to the end of the experiment (Figure 11). By the first sampling occasion, the Eh in the eluate was on average (of the column duplicates) -61 mV. To the second sampling occasion, the Eh decreased sharply and remained stable on average -181 mV from the second sampling occasion to the end of the experiment.

The first sampling occasion, the pH in the eluate from the mZVI duplicates was average 7.6 (of the column duplicates), and increased to the second sampling occasion to average 8.4 around where it remained stable to the end of the experiment (Figure 11). By the first sampling occasion, the Eh in the eluate was positive, at an average of (of the column duplicates) +89 mV. To the second sampling occasion, the Eh decreased sharply to average -152 mV. The Eh decreased further to the fourth sampling occasion to average -205 mV, around where it remained stable to the end of the experiment.

The first sampling occasion, the pH in the eluate from the nZVI duplicates was average 8.2 (of the column duplicates), and increased to the second sampling occasion to average 8.5 around where it remained stable to the end of the experiment (Figure 11). By the first sampling occasion, the Eh in the eluate was on average (of the column duplicates) -99 mV. To the second sampling occasion, the Eh decreased sharply to -202 mV. From sampling occasion three to the end of the experiment, the Eh fluctuated between -193 mV and -160 mV, with an average of -175 mV.

Comparison to reference column

As compared to the reference column, S-nZVI, mZVI and nZVI had clearly increased pH of the system by the second sampling, and to a more stable pH. S-mZVI initially increased pH of the system by the second sampling, but after 340 PV, pH remained stable around a lower pH which was very similar to the reference.

As compared to the reference column, Eh was clearly lowered by S-nZVI, mZVI and nZVI by the second sampling. mZVI initially increased Eh by the first sampling, as compared to the reference. After the decreased Eh, it was similarly to pH kept relatively stable in these treated columns as compared to the reference. Similarly to mZVI, S-mZVI increased Eh compared to the reference by the first sampling, after which it lowered it. Similarly to its pH-trend, the Eh for S-mZVI

shifted again by 340 PV, to higher values. These were inside the Eh range of the reference. This sorbent also stabilized Eh as compared to the reference.

4.3.3. Arsenic

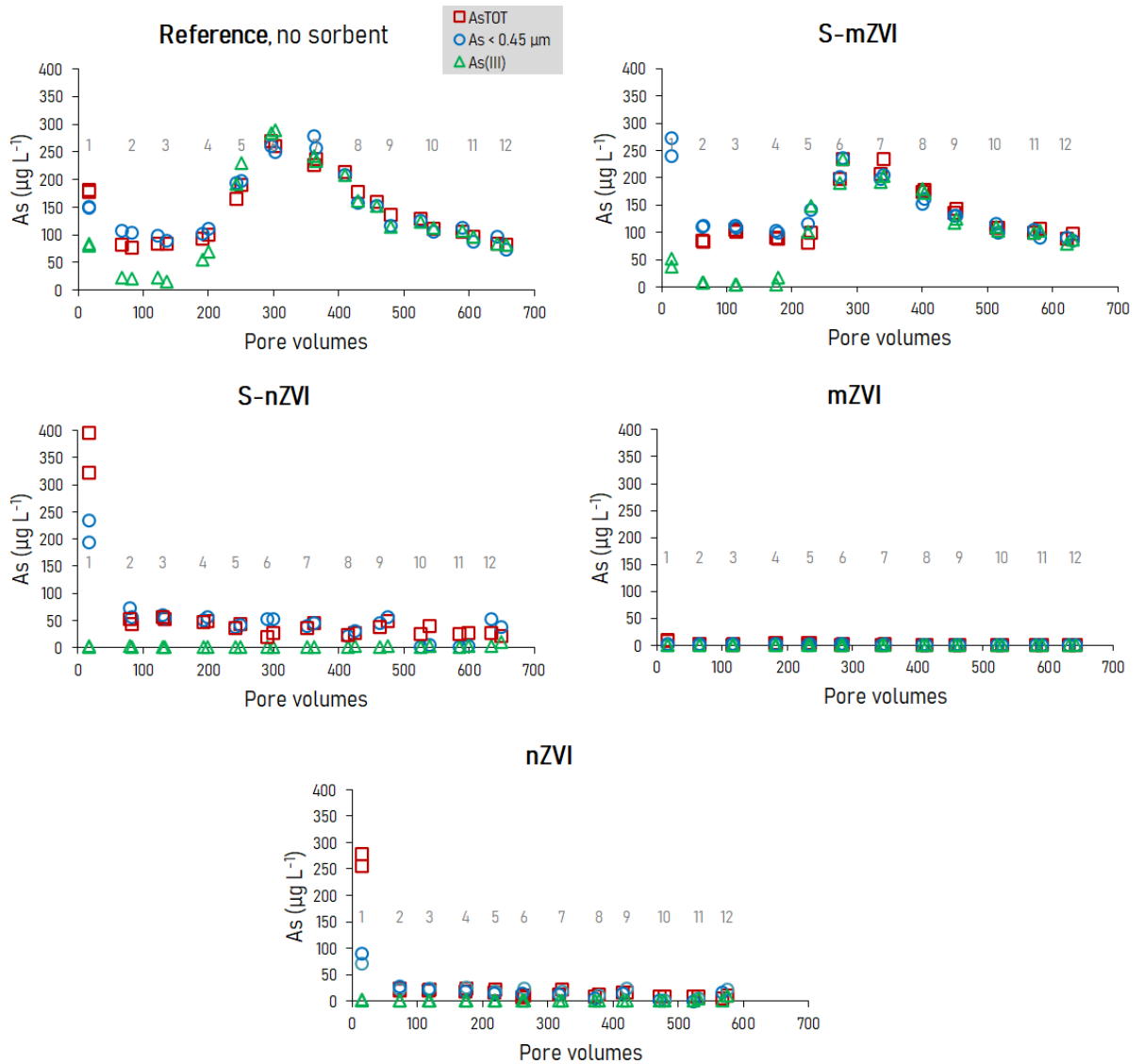


Figure 12. As leaching per respective column type in $\mu\text{g L}^{-1}$. As_{TOT} from respective duplicate shown in red squares, $< 0.45 \mu\text{m}$ fraction from respective duplicate shown in blue circles and As(III) from respective duplicate shown in green triangles. Time of experiment duration is expressed in number of pore volumes passed through respective column type. Samplings are marked with grey numbers 1-12.

The concentration of leached As_{TOT} in the eluate from the reference duplicates decreased from the first sampling occasion to the second from approximately $180 \mu\text{g L}^{-1}$ to approximately $80 \mu\text{g L}^{-1}$ (Figure 12). The following 2 occasions showed a slight increase in leached As_{TOT} per sampling period, and on the fifth sampling

occasion, the leached A_{STOT} increased sharply to close to the initial concentration. The eluate collected from the sixth sampling period contained the highest concentration of A_{STOT} in the experiment, with approximately $265 \mu\text{g L}^{-1}$. Following this peak, the trend of the leached A_{STOT} decreased towards the end of the experiment.

The leached $< 0.45 \mu\text{m}$ fraction (truly dissolved + colloidal) of As from the reference duplicates made up 100 % of the leached A_{STOT} throughout the experiment. The As(III) fraction followed the trend of A_{STOT} and $< 0.45 \mu\text{m}$ fraction leaching, though at lower concentrations from sampling occasion one to four, starting at approximately $80 \mu\text{g L}^{-1}$. Generally, the amount of $< 0.45 \mu\text{m}$ fraction (truly dissolved + colloidal) of As that is not made up by As(III) can be considered As leaching by colloids. From the fifth sampling occasion onward, the A_{STOT} was made up of 100 % of the As(III) fraction. The concentration of As from the final sampling period was $80 \mu\text{g L}^{-1}$.

The concentration of leached A_{STOT} in the eluate from the S-mZVI duplicates decreased very sharply from the first sampling occasion to the second from average $693 \mu\text{g L}^{-1}$ to average $84 \mu\text{g L}^{-1}$ (Figure 12). Note that the A_{STOT} for the first sampling is outside of scale of the figure. The third sampling occasion showed a slight increase in leached A_{STOT} , which was followed by a slightly decreasing trend to the fifth sampling occasion. To the sixth sampling occasion, the leached A_{STOT} concentration in the eluate increased to average (of the column duplicates) $216 \mu\text{g L}^{-1}$. Sampling occasion seven created a plateau (with occasion six) with an average of leached A_{STOT} $222 \mu\text{g L}^{-1}$. Though the concentrations from these sampling occasions differed between the column duplicates noticeably. Because of this difference, the decreasing trend that followed towards the end of the experiment was sharper for one column than for the other.

The leaching evolution for the $< 0.45 \mu\text{m}$ fraction (truly dissolved + colloidal) of As from the S-mZVI duplicates was similar to that of A_{STOT} . The leached $< 0.45 \mu\text{m}$ fraction of As in the eluate decreased sharply from the first sampling to the second from average $256 \mu\text{g L}^{-1}$ to average $112 \mu\text{g L}^{-1}$. The third sampling showed a slight increase in concentration of leached $< 0.45 \mu\text{m}$ fraction of As, which was followed by a slightly decreasing trend. Though this shifted to an increasing trend already at sampling five, to reach a second maximum at the sixth sampling, with an average of $219 \mu\text{g L}^{-1}$. Though the concentrations from this sampling occasion differed between the column duplicates noticeably. Because of this difference, sampling six and seven creates a plateau maximum for one column duplicate and for the other duplicate, an earlier initiation of decreasing trend towards the end of the experiment as compared to the first column.

From the first to the second sampling, the leached As(III) concentration from the S-mZVI duplicates decreased from average $45 \mu\text{g L}^{-1}$ to an average of $9 \mu\text{g L}^{-1}$. This was followed by a minimum plateau to sampling occasion four. This

difference from the concentration of leached $< 0.45 \mu\text{m}$ fraction (truly dissolved + colloidal) of As can be accounted to colloidal leaching of As. From sample occasion five, the leached concentration of As(III) was very similar to that of the $< 0.45 \mu\text{m}$ fraction of As, including the difference between the column duplicates.

The concentration of leached A_{TOT} in the eluate from the S-nZVI duplicates decreased very sharply from the first sampling occasion to the second from average $359 \mu\text{g L}^{-1}$ to average $48 \mu\text{g L}^{-1}$ (Figure 12). The third sampling occasion resulted in a slight increase to average $54 \mu\text{g L}^{-1}$, to be followed by a decreasing trend to sampling occasion 6 when the concentration was $23 \mu\text{g L}^{-1}$ on average. Then followed an alteration in slight increase and decrease every other sampling occasion to the ninth sampling occasion. This was followed by a decreasing trend towards the end of the experiment.

The leaching evolution for the $< 0.45 \mu\text{m}$ fraction (truly dissolved + colloidal) of As from the S-nZVI duplicates was similar to that of A_{TOT} , though showed the opposite direction for some sampling occasions. The leached $< 0.45 \mu\text{m}$ fraction of As in the eluate decreased sharply from the first sampling occasion to the second from average (of the column duplicates) $215 \mu\text{g L}^{-1}$ to average $64 \mu\text{g L}^{-1}$. The first deviation from the A_{TOT} trend was shown at sampling occasion six where there was a slight increase in the leached $< 0.45 \mu\text{m}$ fraction of As. The concentration was $53 \mu\text{g L}^{-1}$. The second deviation from the A_{TOT} trend was at sampling occasion 10 and 11 where the leached $< 0.45 \mu\text{m}$ fraction of As was on average $3 \mu\text{g L}^{-1}$. The last deviation from the A_{TOT} trend was the last (12th) sampling occasion, where the leached $< 0.45 \mu\text{m}$ fraction of As was average $46 \mu\text{g L}^{-1}$.

The leached As(III) concentration from the S-nZVI duplicates remained stable on average (of the column duplicates for all sample occasions) $2 \mu\text{g L}^{-1}$ throughout the experiment duration. Again, the concentration of leached $< 0.45 \mu\text{m}$ fraction of As that was not made up by As(III) can be accounted to colloidal leaching of As.

The leached concentration in the eluate from the mZVI duplicates remained relatively constant for all fractions of As throughout the experiment, at or below $9 \mu\text{g L}^{-1}$, with an average of 1.9, 0.3 and $1.3 \mu\text{g L}^{-1}$ of column duplicates from all sampling occasions for A_{TOT} , As(III) and $< 0.45 \mu\text{m}$ fraction of As respectively (Figure 12).

The concentration of leached A_{TOT} in the eluate from the nZVI duplicates decreased very sharply from the first sampling occasion to the second from average $267 \mu\text{g L}^{-1}$ to average $22 \mu\text{g L}^{-1}$ (Figure 12). The leached A_{TOT} in the eluate remained stable around that concentration until the fifth sampling occasion, to decrease further at the sixth to average $9 \mu\text{g L}^{-1}$ around where it remained relatively stable to the end of the experiment. The leached $< 0.45 \mu\text{m}$ fraction (truly dissolved + colloidal) of As in the eluate decreased from the first sampling occasion to the second from average (of the column duplicates) $81 \mu\text{g L}^{-1}$ to average $25 \mu\text{g L}^{-1}$, around where it remained relatively stable to the end of the experiment. The leached

concentration of As(III) in the eluate remained relatively constant throughout the experiment, on average $2 \mu\text{g L}^{-1}$ (of column duplicates for all sampling occasions). The concentration of leached $< 0.45 \mu\text{m}$ fraction of As that was not made up by As(III) by the first sampling can be accounted to colloidal leaching of As.

As leaching as compared to reference column

The As leaching from the S-mZVI duplicates was very similar to that from the reference duplicates, except by the first sampling when leached A_{TOT} concentration was much higher for S-mZVI: average $693 \mu\text{g L}^{-1}$ compared to approximately $180 \mu\text{g L}^{-1}$. The initially leached A_{TOT} was made up of about 50/50 particular/truly dissolved + colloidal As. As the leached As(III) concentration was similar to that for the reference columns at this time, the soluble part of this increased leaching was comprised of As(V).

The As leaching from the S-nZVI duplicates was lower than that from the reference duplicates. Except by the first sampling, where leached A_{TOT} was roughly twice as high for S-nZVI, similar behavior to S-mZVI. This initially leached A_{TOT} was made up of about 50/50 particular/truly dissolved + colloidal As. The leached A_{TOT} remained around $50 \mu\text{g L}^{-1}$ after the initial high leached concentrations, whereas the reference duplicate eluates reached these low concentrations only in the beginning of the experiment and towards the end of the experiment when extensive leaching of the system had been occurring. A_{TOT} consisted to 100 % of soluble As (truly dissolved + colloidal) after the initial increased leaching event. Leached As(III) concentration from the S-nZVI remained much lower than from the reference duplicates, with average $2 \mu\text{g L}^{-1}$ throughout the experiment. The soluble part of the initial increased leaching of As was made up of As(V).

The As leaching from the mZVI duplicates remained relatively constant for all fractions throughout the experiment, at or below $9 \mu\text{g L}^{-1}$.

The As leaching from the nZVI duplicates was lower than from the reference duplicates (at or below $25 \mu\text{g L}^{-1}$), except the first sampling when leached A_{TOT} concentration was average $267 \mu\text{g L}^{-1}$ (compared to $180 \mu\text{g L}^{-1}$ from the reference duplicates). Hence, leaching behavior was similar to that from S-mZVI and S-nZVI. A majority of A_{TOT} at this leaching event was made up of particulate leaching. As(III) remained on average $2 \mu\text{g L}^{-1}$ throughout the experiment. Hence, the soluble part of the initial leaching of As was made up of As(V).

Mass balance

The total amount of leached A_{TOT} for the entire long-term experiment was the largest for the S-mZVI duplicate columns, with an average $1\,319 \mu\text{g}$, corresponding to 31 % of the initial input by the contaminated sediment (Table 6). The second largest A_{TOT} leaching was found for the non-treated duplicate columns (reference).

The remaining treated columns leached A_{STOT} in the following falling order: S-nZVI > nZVI > mZVI.

The A_{STOT} leached from the reference duplicates was 100 % made up of the < 0.45 μm fraction and 95 % of As(III) (Table 6). The A_{STOT} leached from the S-mZVI duplicates was 94 % made up of the < 0.45 μm fraction and 76 % of As(III). The A_{STOT} leached from the S-nZVI duplicates was 93 % made up of the < 0.45 μm fraction and 5.1 % of As(III). The A_{STOT} leached from the nZVI duplicates was 73 % made up of the < 0.45 μm fraction and 6.8 % of As(III). The A_{STOT} leached from the mZVI duplicates was 63 % made up of the < 0.45 μm fraction and 9 % of As(III).

Table 6. Mass balance for leached As for the entire experiment duration for each column type.

Column	Mass balance As leached					
	A_{STOT}		As < 0.45 μm		As(III)	
	(μg)	(% of input by sediment)	(μg)	(% of A_{STOT} leached)	(μg)	(% of A_{STOT} leached)
nZVI	203	4.7	149	73	14	6.8
S-nZVI	430	10	398	93	22	5.1
Reference	1264	31	1310	100	1198	95
mZVI	14	0.3	9	63	1.3	9
S-mZVI	1319	31	1235	94	1005	76

The same masses of leached As as presented above are in Figure 13 presented in % of the total leached masses from the reference duplicates per respective fraction (A_{STOT} , As < 0.45 μm and As(III)). The leached amount from S-mZVI duplicates is very similar to that of the reference column (without treatment) with at least 84 % (As(III)) of what was leached from the reference duplicates. The A_{STOT} and As < 0.45 μm fraction leached from the S-nZVI duplicates was around 30 % of that of the same fractions leached from the reference duplicates, while the As(III) leached was only 1.9 % of the same fraction from the reference duplicates. The leached amount from the nZVI duplicates for A_{STOT} was 16 % of that from the reference duplicates, the As < 0.45 μm fraction was 11 % of that from the reference duplicates and the As(III) fraction was 1.2 % of that from the reference duplicates. The amounts leached from the mZVI duplicates was less than 1.2 % of the amounts leached from the reference duplicates for all fractions.

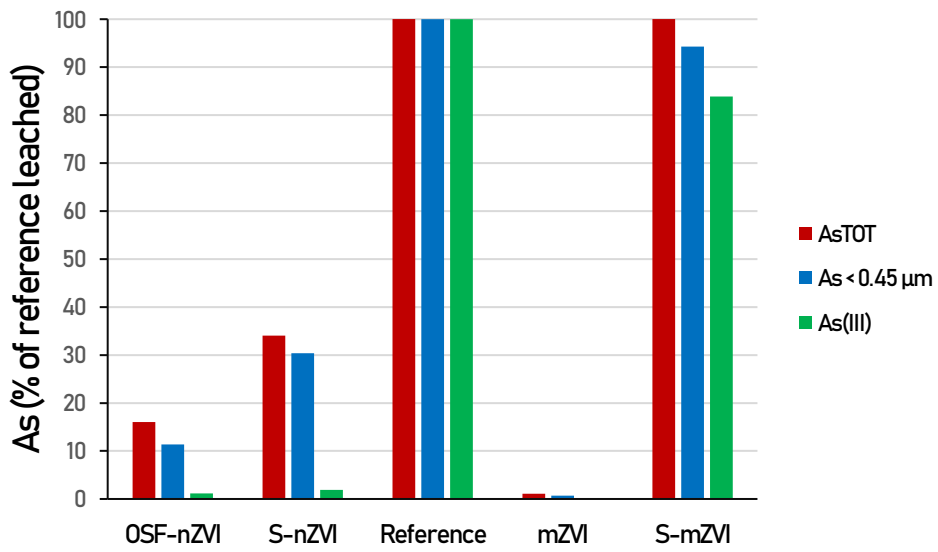


Figure 13. Total amount of leached As during the experiment per column type. Each As fraction amount expressed in % in relation to the corresponding leached amount from the reference duplicates.

5. Discussion

5.1. ICP-MS method development

Using correction equations can be a blunt tool as it is based on *assumptions* made about the components present in the instrument, hence risking to correct for elements that are not present in the instrument. Conversely, they do not correct adequately if the concentration of the interfering element is high. When analyte is at concentrations sub $\mu\text{g L}^{-1}$, using correction equations might become increasingly insufficient (Neubauer 2010). Collision mode or reaction mode settings in the ICP-MS allows for better control of the actual constituents present. When no As was present in the samples, the relative error was not as large possibly because the instrument only detected CaCl^+ and ArCl^+ at $m/z^+ 75$ and the equation (when used) suppressed part of it. When more than $1 \mu\text{g L}^{-1}$ As was present, i.e. $10 \mu\text{g L}^{-1}$, the relative error was smaller because the share of analyte in the sample was higher.

It is known that the As-interfering CaCl^+ at $m/z^+ 75$ is non-reactive with many gases due to the strong bond in the molecule. This makes As-analysis with collision mode in ICP-MS potentially disadvantageous. Here, reaction mode using O_2 which leads to O *readily and rapidly* forming AsO^+ with As, and allows measuring As at $m/z^+ 91$ becomes more reliable (Neubauer 2010).

5.2. Trends of column leaching, pH and Eh as compared to batch tests

Despite the more limited contact time and solute-available particle surface area compared to batch tests, the column tests showed As immobilization by the sorbents which were comparable to batch test results.

5.2.1. Reference

The first decreasing trend in As leaching to the third sampling could be explained by depletion of the mobile As pool available in that time frame. A_{TOT} was 100 % comprised of the $< 0.45 \mu\text{m}$ fraction (truly dissolved + colloidal) throughout the

experiment, and in this first depletion period, the dominating speciation was As(V), likely colloiddally bound. The increase in leached concentration of A_{STOT} from the reference columns following this initial decrease (after third sampling) could be explained by reduction of sediment-bound As(V) to As(III) due to the anoxic conditions. This reduction to the more mobile As species is slow and would explain why there is a lag in the As leaching from experiment start. The total leached As(III) amount made up 95% of A_{STOT} . It has been suggested that mobilization of As(III) that has been reduced from As(V) in reducing conditions while bound in soil additionally calls for reductive dissolution of the Fe(hydr)oxides of the soil (Dixit and Hering 2003). Though there was no clear trend in increasing Fe leaching in relation to this. When the leached A_{STOT} concentration started decreasing after 300 PV, the As available for desorption from the sediment during the time frame was probably desorbed and continuously leached out, towards depletion of the available As in the column. This shows the de-saturation of the system which is inherent with the column method.

The previously performed batch tests showed an increased mobilization of A_{STOT} and increased share of As(III) with time (time frame was 20 days shorter for batch tests) (Figure 2), which is agreeing with what was observed in the results from the columns in the current study. The fact that there was no decrease in mobilized As concentration towards the end of the batch tests, as it was for the column tests, is inherent by the way the method is designed. Because, as stated in section 2.4.1, the As saturation of the closed batch system does not change.

5.2.2. S-mZVI

The S-mZVI columns in the current study showed that the sorbent actually initially increased the mobilization of As as compared to the reference state. The difference in leaching of soluble As to that from the reference was mostly made up of As(V) (likely colloiddally bound), indicating that the sorbent had oxidized and/or immobilized As(III), mediated by the Fe^{2+} formed upon the sorbent corrosion. This prevalence of As(V) could also be observed in the previously performed batch tests (Figure 2). Half of A_{STOT} was made up of As > 0.45 μm during the column test, hence, As was possibly leached out while sorbed to sorbent aggregates and/or sorbent corrosion products.

After the initial increased mobilization of As, the S-mZVI column leaching trend looked very similar to the one for the columns without any treatment. Looking at the Fe leaching from the S-mZVI columns, the initial immense Fe loss (77 times higher than reference, and a majority particulate) could mean significant loss of the amount of sorbent that was initially added to each column, which was why the As leaching behavior of the column system then merged with that of the reference column. Indeed, looking at the Fe mass balance for the S-mZVI columns, 93% of the Fe added through the sorbent was lost. Additionally, looking at pH and Eh

measurements for S-mZVI, these clearly shift to reference-state after 340 PV. This coincides with the time point when leached As concentration reached its maximum.

In summary: The effect from the S-mZVI that could be observed in the column tests was the oxidation and/or immobilization of the soluble As(III) by the first sampling, after which the majority of the sorbent input was leached out. The total amount of leached As in proportion to As input by sediment was the same from the S-mZVI columns as it was for the reference columns, hence, it did not immobilize As in this experiment.

Conversely, the batch tests showed that S-mZVI did immobilize As from a contact time longer than 0 days. The large discrepancy between the test results is due to that the sorbent was not lost from the batch system, because these systems are closed.

The mobilization of the S-mZVI sorbent that was so distinguishable as compared to the other sorbents could likely be explained by the stabilizer added to the product (section 3.4). Additionally, the sulfidated coating could lead to a slightly higher surface charge as compared to its non-sulfidated counterpart.

5.2.3. S-nZVI

Similarly to S-mZVI, the S-nZVI columns in the current study showed that the sorbent actually initially increased the mobilization of As as compared to the reference state. The absolute majority of the soluble fraction consisted of As(V) throughout the experiment duration (possibly colloidally bound), which was also observed in the previously performed batch tests. This indicated that the sorbent oxidized and/or immobilized As(III). Similarly to S-mZVI, this initial increased mobilization of As was coupled with increased leaching of Fe (four times higher than that from reference, and a majority in particulate fraction), indicating that there was a loss of sorbent from the column also for the S-nZVI duplicates.

Following the initial increased mobilization, As was immobilized, especially shown by the fact that the increased As leaching that was visible from the reference columns after the fourth sampling was suppressed by the sorbent. The leached As concentration rather remained on an even and lower level throughout the experiment duration, comprised in majority of soluble As. Similarly, the mobilized As in the corresponding batch tests remained on a relatively even level irrespective of contact time, lower than the reference, showing successful immobilization.

With time, there was an increase in leached concentration of Fe (starting at lower level than first sampling) which was about twice the level of the reference state, and fully comprised of the soluble fraction. Hence within this time frame, Fe was lost without losing the immobilizing effect of As. Fe mass balance for the entire experiment duration indicate that 10 % of the added Fe through sorbent was lost.

The initial increased mobilization of As was not observed in the corresponding batch tests. This supports the hypothesis that the increased mobilization of As from

the columns was because of sorbent loss and As bound to these leaching out along with them, because the closed batch systems can not loose system constituents.

Eh and pH clearly stabilized at lower respectively higher values as compared to the reference state, which could be indicative of Fe(0) corrosion of the sorbent (Wang et al 2021).

5.2.4. mZVI

As was extensively immobilized by mZVI, as leached concentrations remained below $9 \mu\text{g L}^{-1}$ throughout the experiment duration. This is below the Swedish guideline value for As in drinking water ($10 \mu\text{g L}^{-1}$ (Kemakta konsult AB & Institutet för Miljömedicin 2011)). This is in agreement with what was observed in the corresponding batch tests. There was an increase in leached concentration of Fe as compared to the reference from the third sampling, fully comprised of the soluble fraction. Hence Fe was lost without losing the immobilizing effect of As.

After the third sampling was when Eh and pH reached the values where they remained stable throughout the experiment duration, lower respectively higher than the reference. This could indicate Fe(0) corrosion (Wang et al 2021). Fe mass balance indicate that only 1 % of the Fe that was added to the column by the sorbent was lost during the experiment. Hence, out of all sorbents tested, this was the one that was leached out to the lowest degree. Additionally, the amounts As leached from the mZVI duplicates was the lowest for all tested sorbents, with less than 1.2 % of the amounts leached from the reference duplicates for all fractions.

5.2.5. nZVI

Similarly to S-mZVI and S-nZVI, nZVI actually initially increased mobilization of As as compared to the reference state. The speciation of the soluble fraction of this initial mobilization was almost exclusively As(V) (possibly colloidal). A_{TOT} was majorly made up of particulate As, hence, a large part of As was possibly leached out while sorbed to sorbent aggregates and/or sorbent corrosion products. Coinciding with this was an initial increased leached Fe concentration, 10 times higher than the reference state (and a majority particulate). This is again indicative of leaching of sorbent or corrosion products of the sorbent.

Following the initial increased mobilization, As was immobilized, as the increased As leaching that was visible from the reference columns after the fourth sampling was suppressed by the sorbent. The leached As concentration rather remained on an even and lower level throughout the experiment duration, at or below $25 \mu\text{g L}^{-1}$. Hence, the sorbent immobilized As, though the solution concentration exceeded the Swedish guideline value for As in drinking water, $10 \mu\text{g L}^{-1}$ (Kemakta konsult AB & Institutet för Miljömedicin 2011). In the

corresponding batch tests, As was completely immobilized irrespective of contact time.

Similarly to S-nZVI, with time, there was an increase in leached concentration of Fe (starting at lower level than first sampling) compared to the reference state, comprised for the most part by the soluble fraction. Though, as with S-nZVI, within this time frame, Fe was lost without losing the immobilizing effect of As. Fe mass balance for the entire experiment duration indicate that 9 % of the added Fe through sorbent was lost. The Fe leaching from nZVI was only slightly smaller than that from S-nZVI, hence not owing such large difference in sorbent mobility due to higher surface charge because of the sulfide coating of the latter (as seen in the micro sorbents). This could point towards the stabilizer added exclusively to the S-mZVI being the major cause for the mobility of the sorbent, rather than the slightly higher surface charge.

The initial increased mobilization of As was not observed in the corresponding batch tests. This supports the hypothesis that the increased mobilization from the columns was because of sorbent loss and As bound to the sorbent leaching out with these, because the closed batch systems can not loose system constituents.

Eh and pH stabilized at lower respectively higher values than the reference state by the second sampling, this could indicate corrosion of Fe(0) (Wang et al 2021).

5.3. Long-term reactivity of sorbents toward As(III) and As(V)

The efficiency of A_{TOT} immobilization (in comparison to the reference state) by the sorbents were in the falling order: mZVI > nZVI > S-nZVI >> S-mZVI. Though because of the loss and coupled inability to see the effect of S-mZVI, this sorbent should possibly be ruled out. The order of efficiency agrees with the results from the batch tests. Both of these investigations underline the better suitability of non-sulfidated ZVI at Hjärtevad. Hence, the hypothesis of the study was disproven.

If a sorbent showed good performance for a majority of the time, but not until after some degree of increased As mobilization, this might not be as viable an option as another. By looking at mass balance for As for the entire experimental duration, this is taken into account. On a total, the reference column system retained 61 % of its As. The mZVI column system retained 99.7 % of its As, without initial increased mobilization of As. The nZVI column system retained 95.3 % of its As, with initial increased mobilization of As. The S-nZVI column system retained 90 % of its As, with initial increased mobilization of As (higher than that of the nZVI system). Hence, the non-sulfidated sorbents performed well to the end of the experiment duration, indicating efficient As immobilization for 3.4 years at Hjärtevad.

mZVI immobilized As(III) and As(V) to the same extent and kept A_{TOT} in solution below the Swedish guideline value for As in drinking water $10 \mu\text{g L}^{-1}$. Where immobilization of As was not complete i.e. for nZVI and S-nZVI, As(III) leaching was suppressed to a greater extent than As(V), especially by the first sampling.

5.4. Suggested mechanisms for mZVI, nZVI and S-nZVI

Due to the increasing electrostatic repulsion between ZVI surface and both As(III) and As(V) aqueous species at $\text{pH} > 7$ (Kanel et al 2005, Tanboonchuy et al 2011), sorption in the investigated systems could be more favorable on Fe(hydr)oxide/corrosion products of the ZVIs. Because hydroxide formation of Fe(III) is favored at high pH systems (Schmid et al 2015), it is possible that this was the dominating hydroxide type formed after the corrosion as expected had increased the system pH (Wang et al 2021), with example green rust (commonly formed in anoxic conditions at pH 4-10) (Randall et al 2001, Kumar et al 2014). Magnetite is also formed in anoxic conditions (Wang et al 2021). Both are known to sorb As(V) well, though the strongest at pH 7 (Usman et al 2018). As(III) sorption to magnetite increases with pH in the range prevalent in this experiment (even up to 9.5), which could explain its low concentration in solution (Dixit and Hering 2003). For the column systems of mZVI, nZVI and S-nZVI, pH remained at 8.5. Additionally, As(V) speciation was favored over As(III) by the increased pH of the systems. The increased pH caused by ZVI corrosion might have caused increased desorption of (mainly) As(V) from sediment sorption sites, depending on the type of Fe(hydr)oxide that is found in the Hjärtevad soil.

Since the corrosion of the ZVI and system continuously were in anoxic conditions in this experiment, it is probable that less ordered Fe(hydr)oxides were formed and remained stable, hence providing more sorption sites per mass Fe(hydr)oxides as compared to a system where more ordered structures of Fe(hydr)oxides would be formed (Smedley and Kinniburgh 2002). This is favorable for adsorption as removal mechanism, mainly affecting As(V) sorption (Smedley and Kinniburgh 2002).

As observed for S-nZVI, mZVI and nZVI: The increasing leaching of soluble Fe with time is an indicator of Fe(0) corrosion of the sorbents, as this releases Fe^{2+} (Wang et al 2021). As the Fe leaching during effective As immobilization was dominated by soluble Fe, it could be hypothesized that the corrosion of ZVI released some dissolved amount of Fe^{2+} , subsequently forming Fe(hydr)oxides that could sorb As (possibly of Fe(III) type as stated above). As the sorbed As was kept

in the system, the continuous corrosion of the Fe(0) core would exclusively leach out part of the continuously formed Fe²⁺.

nZVI is expected to sorb As to a higher degree than mZVI per amount of added sorbent due to higher specific surface area (Wang et al 2021). The fact that mZVI immobilized As to a higher degree in this study might be explained by aggregation of the nZVI which would decrease the availability to the sorption sites, or it could indicate that sorption was not the main removal mechanism in the experiment. Possibly more importantly, the dosage was four times higher for mZVI than for the other sorbents, and this could be a large contributor to its higher efficiency observed in the experiment. Coprecipitation with Fe(hydr)oxides is rather the likely removal mechanism, which is less sensitive to change in pH and competing anions than the inner-sphere complexes are.

Reduction of As(III) to the less soluble As(0) is not expected by mZVI (Yan et al 2012), hence, its great immobilization of As(III) in this study is not probably due to this mechanism. Additionally pH 8.5 and Eh -200 mV is rather at the border between the predominance regions for As(III) and As(V) (Figure 1), hence, presence of As(0) is less likely.

Mechanisms S-nZVI

Similar to what Singh et al (2021) and Wu et al (2018) observed, As(III) concentration in solution was lowered by S-nZVI in anoxic conditions.

Wu et al (2018) observed higher removal rate for S-nZVI than for regular nZVI in pH 3-9, which was not observed in this study, disproving the hypothesis stated. The total leaching of Fe for the two sorbents were very similar in this study, and the discrepancy to the results from Wu et al (2018) could therefore not be explained by the loss of sorbent. Though the difference in removal capacity of S-nZVI and regular nZVI was larger in oxic conditions as compared to anoxic, which were prevalent in this study. Hence regular nZVI might have been more efficient in the predominantly anoxic conditions in the current study.

Sorption has been suggested to be an important removal mechanism for As by S-nZVI (Singh et al 2021, Wu et al 2018). With higher pH, adsorption might become an even more important removal mechanism for S-nZVI (Singh et al 2021), and if these sites are blocked by the coating, the efficiency of the sorbent can be noticeably hampered (Phenrat et al 2009). The S-nZVI surface can also be passivated by precipitation of Fe oxide in alkaline pH, further hampering As interaction (Singh et al 2021). As the system in the current study shifted and remained stable at pH 8.5, these facts might further explain why efficiency was lower for S-nZVI than for nZVI. Indeed, Singh et al (2021) observed at pH 8 and 9, that removal by S-nZVI of both As(III) and As(V) was significantly poorer than at pH 7. Additionally, sorption of mainly As(V) to the S-nZVI particle decreases with increasing pH similarly to nZVI due to increasing electrostatic repulsion with

the increasingly negatively charged particle surface along with increasingly negatively charged aqueous As species (Singh et al 2021).

Despite As(V) generally sorbing to Fe(hydr)oxides to a greater extent than As(III), As(V) was the main speciation of the soluble As that was leached out. A possible explanation to this could be sorbing to Fe(hydr)oxide colloids which were then leached out. Though, to assess an expected extent of retention by sorption of As(V) in the system, modelling would be required.

It has been suggested that studies on ZVI in certain conditions that have initially been performed in lab-scale in junction of a successive study on pilot- and field-scale should all be compared in a follow-up study in order to try elucidate how representative the lab-scale tests are for ZVI efficiency. As this present study is followed by such pilot- and field-scale application, this could be a possible finalizing step of the series of studies of Hjärtevad.

6. Conclusions

The long-term efficiency of As immobilization by S-nZVI, nZVI, S-mZVI and mZVI in sandy sediment was studied through a percolation experiment in columns under anoxic conditions, and showed that non-sulfidated ZVI have higher potential to perform well in the Hjärtevad aquifer. Hence, the hypothesis of the study was disproven.

mZVI (Ferox Target, Hepure) is suggested as sorbent for immobilizing As in the Hjärtevad aquifer. Recommendation of sorbent in this study is purely done in respect to long-term efficiency toward As immobilization once the sorbent is already in the Hjärtevad subsurface. Hence, delivery issues due to larger particle size of micro-sized ZVI or due to colloidal nature of nano-sized ZVI, or stability of either of the alternatives' solutions are outside the scope of this study.

A final conclusion of suitability of ZVI for Hjärtevad should include consideration of subsurface-delivery challenges and total costs. Extended column studies with changing conditions could solidify the foresight of the long-term immobilization of As by ZVI in Hjärtevad, by for example changing eluent to a solution of certain concentration of As(III), or adjusting the pH of the AGW.

Follow-up studies after executed pilot-test and actual full-scale operation could entail monitoring actual As immobilization and coupling back to precedent lab-scale test results in order to verify the credibility of future batch and column testing of ZVI performance.

The optimal method for analyzing sub $\mu\text{g L}^{-1}$ concentrations of As with ICP-MS was found to be reaction mode using O_2 gas. Optimal design of column testing for sandy soil with ZVI included removal of original filters, followed by addition of 70 μm Nylon mesh filter on both ends, without induced aggregation of nZVI.

References

- Andreottola, G., Bonomo, L. & Pollice, A. (1997). *Comparison of Batch Completely Mixed and Column Tests for the Evaluation of Phenol Mobility in Natural Soils*. Environmental Technology, 18(10), 1037–1044. <https://doi.org/10.1080/09593331808616623>
- Bang, S., Johnson, M.D., Korfiatis, G.P. & Meng, X. (2005b). *Chemical reactions between arsenic and zero-valent iron in water*. Water Research, 39(5), 763–770. <https://doi.org/10.1016/j.watres.2004.12.022>
- Bang, S., Korfiatis, G.P. & Meng, X. (2005a). *Removal of arsenic from water by zero-valent iron*. Journal of Hazardous Materials, 121(1), 61–67. <https://doi.org/10.1016/j.jhazmat.2005.01.030>
- Bowell, R.. (1994). Sorption of arsenic by iron oxides and oxyhydroxides in soils. Applied Geochemistry, 9(3), 279–286. [https://doi.org/10.1016/0883-2927\(94\)90038-8](https://doi.org/10.1016/0883-2927(94)90038-8)
- Bowell, R.J., Alpers, C.N., Jamieson, H.E., Nordstrom, D.K. & Majzlan, J. (2014). *The environmental Geochemistry of Arsenic - An Overview*. Reviews in Mineralogy and Geochemistry, 79(1), 1–16. <https://doi.org/10.2138/rmg.2014.79.1>
- Brumovský, M., Filip, J., Malina, O., Oborná, J., Sracek, O., Reichenauer, T.G., Andrýsková, P. & Zbořil, R. (2020). *Core–Shell Fe/FeS Nanoparticles with Controlled Shell Thickness for Enhanced Trichloroethylene Removal*. ACS Applied Materials & Interfaces, 12(31), 35424–35434. <https://doi.org/10.1021/acsami.0c08626>
- Brumovský, M., Oborná, J., Lacina, P., Hegedüs, M., Sracek, O., Kolařík, J., Petr, M., Kašlík, J., Hofmann, T. & Filip, J. (2021). *Sulfidated nano-scale zerovalent iron is able to effectively reduce in situ hexavalent chromium in a contaminated aquifer*. Journal of Hazardous Materials, 405, 124665. <https://doi.org/10.1016/j.jhazmat.2020.124665>
- Catalano, J.G., Park, C., Fenter, P. & Zhang, Z. (2008). *Simultaneous inner- and outer-sphere arsenate adsorption on corundum and hematite*. Geochimica et Cosmochimica Acta, 72(8), 1986–2004. <https://doi.org/10.1016/j.gca.2008.02.013>
- Cheng, S., Liu, H., Anang, E., Li, C. & Fan, X. (2021). *Enhanced As(III) sequestration using nanoscale zero-valent iron modified by combination of loading and sulfidation: characterizations, performance, kinetics and mechanism*. Water Science and Technology, 83(12), 2886–2900. <https://doi.org/10.2166/wst.2021.184>

- Colon, M., Hidalgo, M. & Iglesias, M. (2009). *Correction strategies over spectral interferences for arsenic determination in aqueous samples with complex matrices by quadrupole ICP-MS*. *Journal of Analytical Atomic Spectrometry*, 24 (4), 518–521. <https://doi.org/10.1039/b820898k>
- Dixit, S. & Hering, J.G. (2003). *Comparison of Arsenic(V) and Arsenic(III) Sorption onto Iron Oxide Minerals: Implications for Arsenic Mobility*. *Environmental Science & Technology*, 37(18), 4182–4189. <https://doi.org/10.1021/es030309t>
- Dunlop, D.. & Özdemir, Ö. (2015). *5.08 - Magnetizations in Rocks and Minerals*. *Treatise on Geophysics*. Second Edition. Elsevier B.V, 255–308. <https://doi.org/10.1016/B978-0-444-53802-4.00102-0>
- Environmental Monitoring Systems Laboratory, U.S. EPA (1996). Method 200.8 - determination of trace elements in waters and wastes by inductively coupled plasma - Mass spectrometry. *Methods for the Determination of Metals and Inorganic Chemicals in Environmental Samples*. 88–145. <https://doi.org/10.1016/B978-0-8155-1398-8.50011-2>
- Essington, M.E. (2015). *Soil and water chemistry : an integrative approach*. Second edition. Boca Raton, FL: CRC Press, an imprint of Taylor and Francis. <https://doi.org/10.1201/b18385>
- Fan, D., Lan, Y., Tratnyek, P.G., Johnson, R.L., Filip, J., O’Carroll, D.M., Nunez Garcia, A. & Agrawal, A. (2017). *Sulfidation of Iron-Based Materials: A Review of Processes and Implications for Water Treatment and Remediation*. *Environmental Science & Technology*, 51(22), 13070–13085. <https://doi.org/10.1021/acs.est.7b04177>
- Gil-Díaz, M., Diez-Pascual, S., González, A., Alonso, J., Rodríguez-Valdés, E., Gallego, J.. & Lobo, M.. (2016). *A nanoremediation strategy for the recovery of an As-polluted soil*. *Chemosphere*, 149, 137–145. <https://doi.org/10.1016/j.chemosphere.2016.01.106>
- Grathwohl, P. & Susset, B. (2009). *Comparison of percolation to batch and sequential leaching tests: Theory and data*. *Waste Management*, 29(10), 2681–2688. <https://doi.org/10.1016/j.wasman.2009.05.016>
- Hao, L., Liu, M., Wang, N. & Li, G. (2018). *A critical review on arsenic removal from water using iron-based adsorbents*. *RSC Advances*, 8(69), 39545–3956. <https://doi.org/10.1039/c8ra08512a>
- Helldén, J., Juvonen, B., Liljedahl, T., Broms, S. & Wiklund, U. (2006). *Åtgärdslösningar – erfarenheter och tillgängliga metoder*. (5637). Stockholm: Naturvårdsverket. <https://www.naturvardsverket.se/om-oss/publikationer/5900/samlad-kunskap-fran-hallbar-sanering/> [2022-01-25]
- Hepure (2021). *Ferox Target Zero Valent Iron powder – sized for source area treatment*. <https://hepure.com/products/ferox-target/> [2022-03-26]
- Kalbe, U., Berger, W., Simon, F.-G., Eckardt, J. & Christoph, G. (2007). *Results of interlaboratory comparisons of column percolation tests*. *Journal of*

- Hazardous Materials, 148(3), 714–720.
<https://doi.org/10.1016/j.jhazmat.2007.03.039>
- Kanel, S.R., Manning, B., Charlet, L. & Choi, H. (2005). *Removal of Arsenic(III) from Groundwater by Nanoscale Zero-Valent Iron*. Environmental Science & Technology, 39(5), 1291–1298.
<https://doi.org/10.1021/es048991u>
- Kemakta Konsult AB & Institutet för Miljömedicin (2011). *Datablad för arsenik* (Rev.ed). <https://www.naturvardsverket.se/vagledning-och-stod/forenaded-omraden/riktvarden-for-forenaded-mark/uppdaterat-berakningsverktyg-och-nya-riktvarden-for-forenaded-mark> [2022-01-27]
- Krüger, O., Kalbe, U., Berger, W., Nordhauß, K., Christoph, G. & Walzel, H.-P. (2012). *Comparison of Batch and Column Tests for the Elution of Artificial Turf System Components*. Environmental Science & Technology, 46(24), 13085–13092. <https://doi.org/10.1021/es301227y>
- Kuhlmeier, P.D. (1997). *Partitioning of Arsenic Species in Fine-Grained Soils*. Journal of the Air & Waste Management Association (1995), 47(4), 481–490. <https://doi.org/10.1080/10473289.1997.10464415>
- Kumar, N., Auffan, M., Gattacceca, J., Rose, J., Olivi, L., Borschneck, D., Kvapil, P., Jublot, M., Kaifas, D., Malleret, L., Doumenq, P. & Bottero, J.-Y. (2014). *Molecular Insights of Oxidation Process of Iron Nanoparticles: Spectroscopic, Magnetic, and Microscopic Evidence*. Environmental Science & Technology, 48 (23), 13888–13894.
<https://doi.org/10.1021/es503154q>
- Kumpiene, J., Carabante, I., Kasiuliene, A., Austruy, A. & Mench, M. (2021). *LONG-TERM stability of arsenic in iron amended contaminated soil*. Environmental Pollution, 269, 116017–8.
<https://doi.org/10.1016/j.envpol.2020.116017>
- Leicht, K. (2021). *Remediation of an arsenic-contaminated anoxic aquifer in Hältevad with zerovalent iron assessment and modelling of sorption strength and solubility of arsenic*. (Master Thesis, 2021:11). Uppsala: Sveriges Lantbruksuniversitet. Department of Soil and Environment/European Master in Environmental Science.
<https://stud.epsilon.slu.se/17362/>
- Li, S., Wang, W., Liu, Y. & Zhang, W. (2014). *Zero-valent iron nanoparticles (nZVI) for the treatment of smelting wastewater: A pilot-scale demonstration*. Chemical Engineering Journal, 254, 115–123.
<https://doi.org/10.1016/j.cej.2014.05.111>
- Li, X., Elliott, D.W. & Zhang, W. (2006). *Zero-Valent Iron Nanoparticles for Abatement of Environmental Pollutants: Materials and Engineering Aspects*. Critical Reviews in Solid State and Materials Sciences, 31(4), 111–122. <https://doi.org/10.1080/10408430601057611>
- Liu, W., Tian, S., Zhao, X., Xie, W., Gong, Y. & Zhao, D. (2015). *Application of Stabilized Nanoparticles for In Situ Remediation of Metal-Contaminated*

- Soil and Groundwater: a Critical Review*. Current Pollution Reports, 1(4), 280–291. <https://doi.org/10.1007/s40726-015-0017-x>
- Lopez Meza, S., Garrabrants, A.C., van der Sloot, H. & Kosson, D.S. (2008). *Comparison of the release of constituents from granular materials under batch and column testing*. Waste Management, 28(10), 1853–1867. <https://doi.org/10.1016/j.wasman.2007.11.009>
- Löv, Å., Larsbo, M., Sjöstedt, C., Cornelis, G., Gustafsson, J.P. & Kleja, D.B. (2019). *Evaluating the ability of standardised leaching tests to predict metal(loid) leaching from intact soil columns using size-based elemental fractionation*. Chemosphere, 222, 453–460. <https://doi.org/10.1016/j.chemosphere.2019.01.148>
- Mamindy-Pajany, Y., Hurel, C., Marmier, N. & Roméo, M. (2011). *Arsenic (V) adsorption from aqueous solution onto goethite, hematite, magnetite and zero-valent iron: Effects of pH, concentration and reversibility*. Desalination, 281(1), 93–99. <https://doi.org/10.1016/j.desal.2011.07.046>
- Manning, B.A., Fendorf, S.E. & Goldberg, S. (1998). *Surface Structures and Stability of Arsenic(III) on Goethite: Spectroscopic Evidence for Inner-Sphere Complexes*. Environmental Science & Technology, 32(16), 2383–2388. <https://doi.org/10.1021/es9802201>
- Martin, M., Violante, A., Ajmone-Marsan, F. & Barberis, E. (2014). *Surface Interactions of Arsenite and Arsenate on Soil Colloids*. Soil Science Society of America Journal, 78(1), 157–170. <https://doi.org/10.2136/sssaj2013.04.0133>
- Mondino, F., Piscitello, A., Bianco, C., Gallo, A., D'Auris, A. de F., Tosco, T., Tagliabue, M. & Sethi, R. (2020). *Injection of Zerovalent Iron Gels for Aquifer Nanoremediation: Lab Experiments and Modeling*. Water, 12(3), 1–15. <https://doi.org/10.3390/w12030826>
- Naka, A., Yasutaka, T., Sakanakura, H., Kalbe, U., Watanabe, Y., Inoba, S., Takeo, M., Inui, T., Katsumi, T., Fujikawa, T., Sato, K., Higashino, K. & Someya, M. (2016). *Column percolation test for contaminated soils: Key factors for standardization*. Journal of Hazardous Materials, 320, 326–340. <https://doi.org/10.1016/j.jhazmat.2016.08.046>
- NANO IRON (2016a). *NANOFER 25S Safety Data Sheet*. <https://nanoiron.cz/en/products/zero-valent-iron-nanoparticles/nanofer-25s> [2022-01-23]
- NANO IRON (2016b). *NANOFER 25DS Safety Data Sheet*.
- Naturvårdsverket (2009a). *Riskbedömning av förorenade områden - En vägledning från förenklad till fördjupad riskbedömning*. (5977). <https://www.naturvardsverket.se/vagledning-och-stod/forenaded-omraden/riskbedomning-av-forenaded-omraden> [2022-01-25]
- Naturvårdsverket (2009b). *Riktvärden för förorenad mark - Modellbeskrivning och vägledning*. (5976). <https://www.naturvardsverket.se/978-91-620-5976-7> [2022-01-28]

- Naturvårdsverket (2021). *Miljömålen - Årlig uppföljning av Sveriges nationella miljömål 2021 – Med fokus på statliga insatser*. (6968).
<https://www.naturvardsverket.se/978-91-620-6968-1> [2022-01-25]
- Naturvårdsverket (2022a). *Inventering av förorenade områden*.
<https://www.naturvardsverket.se/vagledning-och-stod/forenaded-omraden/inventering-av-forenaded-omraden/> [2022-01-27]
- Naturvårdsverket (2022b). *Om förorenade områden*.
<https://www.naturvardsverket.se/amnesomraden/forenaded-omraden/om-forenaded-omraden/> [2022-01-25]
- Naturvårdsverket (2022c). *Antal förorenade områden och Naturvårdsverkets bidrag till inventering, undersökning och åtgärder*.
<https://www.sverigesmiljomal.se/miljomalen/giftfri-miljo/forenaded-omraden/> [2022-03-24]
- Neubauer K. (2010). Reducing the Effects of Interferences in Quadrupole ICP-MS. *Spectroscopy*, 1 November.
<https://www.spectroscopyonline.com/view/reducing-effects-interferences-quadrupole-icp-ms> [2022-01-15]
- Norrfors, K.K., Mici, V., Borovinskaya, O., von der Kammer, F., Hofmann, T. & Cornelis, G. (2021). *A critical evaluation of short columns for estimating the attachment efficiency of engineered nanomaterials in natural soils*. *Environmental Science Nano*, 8(6), 181–1814.
<https://doi.org/10.1039/d0en01089h>
- O’Carroll, D., Sleep, B., Krol, M., Boparai, H. & Kocur, C. (2013). *Nanoscale zero valent iron and bimetallic particles for contaminated site remediation*. *Advances in Water Resources*, 51, 104–122.
<https://doi.org/10.1016/j.advwatres.2012.02.005>
- Phenrat, T., Liu, Y., Tilton, R.D. & Lowry, G.V. (2009). *Adsorbed Polyelectrolyte Coatings Decrease Fe(0) Nanoparticle Reactivity with TCE in Water: Conceptual Model and Mechanisms*. *Environmental science & technology*, 43 (5), 1507–1514.
<https://doi.org/10.1021/es802187d>
- Randall, S.R., Sherman, D.M. & Ragnarsdottir, K.V. (2001). *Sorption of As(V) on green rust (Fe₄(II)Fe₂(III)(OH)₁₂SO₄ · 3H₂O) and lepidocrocite (γ-FeOOH): Surface complexes from EXAFS spectroscopy*. *Geochimica et Cosmochimica Acta*, 65(7), 1015–1023. [https://doi.org/10.1016/S0016-7037\(00\)00593-7](https://doi.org/10.1016/S0016-7037(00)00593-7)
- REGENESIS (2018). *S-MicroZVI Safety Data Sheet*.
<https://regenesisc.com/en/techinfo/regenesisc-safety-data-sheet-sds-center/> [2022-01-23]
- Sadiq, M. (1997). *Arsenic chemistry in soils: An overview of thermodynamic predictions and field observations*. *Water, Air and Soil pollution*, 93 (1), 117–136. <https://doi.org/10.1007/BF02404751>
- Schmid, D., Micić, V., Laumann, S. & Hofmann, T. (2015). *Measuring the reactivity of commercially available zero-valent iron nanoparticles used*

- for environmental remediation with iopromide. *Journal of Contaminant Hydrology*, 181, 36–45. <https://doi.org/10.1016/j.jconhyd.2015.01.006>
- SGI, Swedish Geotechnical Institute (2020). *Forskningsfinansiering inom Tuffo*. <https://www.sgi.se/sv/kunskapscentrum/tuffo-teknikutveckling-fororenade-omraden/> [2022-01-25]
- SGU, Sveriges Geologiska Undersökning (2021). *Beställarnätverket Samverkan för innovation*. <https://www.sgu.se/samhallsplanering/fororenade-omraden/samverkan-for-innovation/> [2022-01-26]
- SGU, Sveriges Geologiska Undersökning (2022). *Avslutade projekt - förorenade områden*. <https://www.sgu.se/samhallsplanering/fororenade-omraden/avslutade-projekt/> [2022-01-26]
- Shi, Z., Fan, D., Johnson, R.L., Tratnyek, P.G., Nurmi, J.T., Wu, Y. & Williams, K.H. (2015). *Methods for characterizing the fate and effects of nano zerovalent iron during groundwater remediation*. *Journal of Contaminant Hydrology*, 181, 17–35. <https://doi.org/10.1016/j.jconhyd.2015.03.004>
- Singh, P., Pal, P., Mondal, P., Saravanan, G., Nagababu, P., Majumdar, S., Labhsetwar, N. & Bhowmick, S. (2021). *Kinetics and mechanism of arsenic removal using sulfide-modified nanoscale zerovalent iron*. *Chemical Engineering Journal*, 412, 128667. <https://doi.org/10.1016/j.cej.2021.128667>
- Sirk, K.M., Saleh, N.B., Phenrat, T., Kim, H.-J., Dufour, B., Ok, J., Golas, P.L., Matyjaszewski, K., Lowry, G.V. & Tilton, R.D. (2009). *Effect of Adsorbed Polyelectrolytes on Nanoscale Zero Valent Iron Particle Attachment to Soil Surface Models*. *Environmental Science & Technology*, 43 (10), 3803–3808. <https://doi.org/10.1021/es803589t>
- Smedley, P. & Kinniburgh, D. (2002). *A review of the source, behaviour and distribution of arsenic in natural waters*. *Applied Geochemistry*, 17(5), 517–568. [https://doi.org/10.1016/S0883-2927\(02\)00018-5](https://doi.org/10.1016/S0883-2927(02)00018-5)
- Sun, Y., Li, J., Huang, T. & Guan, X. (2016). *The influences of iron characteristics, operating conditions and solution chemistry on contaminants removal by zero-valent iron: A review*. *Water Research*, 100, 277–295. <https://doi.org/10.1016/j.watres.2016.05.031>
- SWECO (2019). *Miljöutredning Etapp 2 - Utredning rörande Föroreningsförhållandena vid den f.d. Impregnerings-anläggningen i Hjärtevad, Eksjö kommun*. Sweco Environment AB, pp. 1–185.
- Tanboonchuy, V., Hsu, J.-C., Grisdanurak, N. & Liao, C.-H. (2011). *Impact of selected solution factors on arsenate and arsenite removal by nanoiron particles*. *Environmental Science and Pollution Research International*, 18(6), 857–864. <https://doi.org/10.1007/s11356-011-0442-3>
- Tanchuling, M.A., Khan, M.R.A. & Kusakabe, O. (2005). *Sorption of Zinc in Bentonite, Illite and Kaolin Clay Using Column Leaching Tests. Contaminated Soils, Sediments and Water*. Boston, MA: Springer US, 251–263. https://doi.org/10.1007/0-387-23079-3_16

- Tuček, J., Prucek, R., Kolařík, J., Zoppellaro, G., Petr, M., Filip, J., Sharma, V.K. & Zbořil, R. (2017). *Zero-Valent Iron Nanoparticles Reduce Arsenites and Arsenates to As(0) Firmly Embedded in Core–Shell Superstructure: Challenging Strategy of Arsenic Treatment under Anoxic Conditions*. *ACS Sustainable Chemistry & Engineering*, 5(4), 3027–3038. <https://doi.org/10.1021/acssuschemeng.6b02698>
- U.S. EPA (2004). *Understanding variation in partition coefficient, kd, values, vol. 3, Review of Geochemistry and Available Kd Values for Americium, Arsenic, Curium, Iodine, Neptunium, Radium, and Technetium*. Office of Radiation and Indoor Air, U.S. Environmental Protection Agency, Washington, D.C.
- U.S. EPA (2007). Method 3051A (SW-846): *Microwave Assisted Acid Digestion of Sediments, Sludges, and Oils*. Revision 1. Washington, DC. <https://www.epa.gov/esam/us-epa-method-3051a-microwave-assisted-acid-digestion-sediments-sludges-and-oils> [2022-01-20]
- Usman, M., Byrne, J.M., Chaudhary, A., Orsetti, S., Hanna, K., Ruby, C., Kappler, A. & Haderlein, S.B. (2018). *Magnetite and Green Rust: Synthesis, Properties, and Environmental Applications of Mixed-Valent Iron Minerals*. *Chemical Reviews*, 118 (7), 3251–3304. <https://doi.org/10.1021/acs.chemrev.7b00224>
- Vestin J., Ladekrans T., Ohlsson Y., Stark M. (2021). *Inventering av effektivitetshinder och kunskapsbehov 2021, Förorenade områden – Alternativa åtgärder till schaktsaneringar*. Linköping: Statens geotekniska institut, SGI.
- Wang, S. & Mulligan, C.N. (2006). *Effect of natural organic matter on arsenic release from soils and sediments into groundwater*. *Environmental Geochemistry and Health*, 28(3), 197–214. <https://doi.org/10.1007/s10653-005-9032-y>
- Wang, X., Zhang, Y., Wang, Z., Xu, C. & Tratnyek, P.G. (2021). *Advances in metal(loid) oxyanion removal by zerovalent iron: Kinetics, pathways, and mechanisms*. *Chemosphere*, 280, 130766–130766. <https://doi.org/10.1016/j.chemosphere.2021.130766>
- Wenzel, W. W. (2013) ‘Arsenic’, in Alloway, B. J. (ed.) *Heavy Metals in Soils - Trace Metals and Metalloids in Soils and their Bioavailability*. Third edition. Dordrecht: Springer Netherlands, pp. 241–282. doi: https://doi.org/10.1007/978-94-007-4470-7_9
- WHO (2019). *Preventing disease through healthy environments - exposure to arsenic: a major public health concern*. Geneva: Department of Public Health, Environmental and Social Determinants of Health, WHO. <https://apps.who.int/iris/handle/10665/329482> [2022-01-27]
- Wilschefski, S.C. & Baxter, M.R. (2019). *Inductively Coupled Plasma Mass Spectrometry: Introduction to Analytical Aspects*. *Clinical Biochemist Reviews*, 40(3), 115–133. <https://doi.org/10.33176/AACB-19-00024>

- Wu, D., Peng, S., Yan, K., Shao, B., Feng, Y. & Zhang, Y. (2018). *Enhanced As(III) Sequestration Using Sulfide-Modified Nano-Scale Zero-Valent Iron with a Characteristic Core-Shell Structure: Sulfidation and As Distribution*. ACS sustainable chemistry & engineering, 6(3), 3039–3048. <https://doi.org/10.1021/acssuschemeng.7b02787>
- Yan, W., Lien, H.-L., Koel, B.E. & Zhang, W. (2013). *Iron nanoparticles for environmental clean-up: recent developments and future outlook*. Environmental Science: Processes & Impacts, 15 (1), 63–77. <https://doi.org/10.1039/C2EM30691C>
- Yan, W., Ramos, M.A.V., Koel, B.E. & Zhang, W. (2012). *As(III) Sequestration by Iron Nanoparticles: Study of Solid-Phase Redox Transformations with X-ray Photoelectron Spectroscopy*. Journal of Physical Chemistry C, 116(9), 5303–5311. <https://doi.org/10.1021/jp208600n>
- Yuan, C. and Lien, H.-L. (2006) *Removal of Arsenate from Aqueous Solution Using Nanoscale Iron Particles*. Water Quality Research Journal, 41(2), pp. 210–215. doi: <https://doi.org/10.2166/wqrj.2006.024>
- Zhang, H. & Selim, H.. (2007). *Colloid Mobilization and Arsenite Transport in Soil Columns: Effect of Ionic Strength*. Journal of Environmental Quality, 36 (5), 1273–1280. <https://doi.org/10.2134/jeq2006.0373>
- Zou, Y., Wang, X., Khan, A., Wang, P., Liu, Y., Alsaedi, A., Hayat, T. & Wang, X. (2016). *Environmental Remediation and Application of Nanoscale Zero-Valent Iron and Its Composites for the Removal of Heavy Metal Ions: A Review*. Environmental Science & Technology, 50(14), 7290–7304. <https://doi.org/10.1021/acs.est.6b01897>